ROLE OF SUBSTRATE STIFFNESS IN DRIVING ATHEROGENIC BEHAVIOR IN MACROPHAGES

A Thesis

Presented to the Faculty of the Graduate School

of Cornell University

In Partial Fulfillment of the Requirements for the Degree of

Master of Science

by

Siddhartha Shankar Sinha

May 2014

ABSTRACT

Atherosclerosis is a decades-long process whose patients often remain asymptomatic until after a heart attack or stroke. Novel therapeutic approaches focus on tuning the body's own atheroprotective mechanisms to induce regression. My approach looks at macrophages, which is the most prominent immune cell type in atherosclerotic plaque due to its involvement in lipid clearance, apoptotic cell debris clearance and pro- or anti-inflammatory cytokine production. While the molecular mechanisms active in lesional macrophages have been extensively studied, the effect of age- and inflammation-induced arterial stiffening on macrophage function is not yet fully understood. Thanks to recent advances in bioengineering that provided the tools to mimic physical properties of tissue, the effect of physical stiffness and associated matrix remodeling on macrophages can now be studied. Herein I describe the effects of physical substrate stiffness on macrophage behavior relevant to atherosclerosis plaque formation using a polyacrylamide hydrogel-based *in vitro* model of atherosclerotic tissue.

BIOGRAPHICAL SKETCH

Siddhartha Shankar Sinha was born on September 23rd, 1987 in Sambalpur, Orissa, India. He attended Kendriya Vidyalaya in Puri through Junior High and Deepika E. M. School in Rourkela through Senior High School, during which his interest in the life sciences was kindled and supported by his family, teachers and friends. Siddhartha graduated with honors in May of 2005 and came to the Unites States to attend college at the University of Washington in Seattle, where he pursued his interests in the life sciences and his aptitude in the engineering disciplines under the guidance of many great instructors. He graduated in 2009 with a B.S. in Biomedical Engineering. Siddhartha came to Cornell to carry out his graduate studies in the field of Molecular and Integrative Physiology in the summer of 2011 and joined the lab of Prof. Cynthia Leifer in the summer of 2012. While in Prof. Leifer's lab, he has studied the behavior of macrophages on polyacrylamide gel models of atherosclerotic tissue and earned his M.S. in April 2014.

This thesis is dedicated to my parents Shri Prabhas Krishna Sinha and Dr. Banani Roy, whose ever-present love and support has guided me to success and fulfillment through all my life.

ACKNOWLEDGMENTS

First and foremost I would like to thank my advisor Prof. Cynthia A. Leifer, for whose mentorship I will be forever grateful. Her passion for knowledge and infectious enthusiasm will always be a source of inspiration for me, and her patience and dedication to being my guide has provided me with both the tools necessary to be an independent scientist and a role model for my own future endeavors in teaching and mentorship. Graduate school is a massive undertaking, and her unshakeable faith in me and desire to see me succeed in all my endeavors has guided me safely through many a difficult time.

I would also like to thank my committee members, Prof. Mark S. Roberson and Prof. Robert S. Weiss, for their valuable support and wise guidance throughout my career at Cornell.

I express my sincere thanks to all of my colleagues at the Leifer Lab past and present. Jody Cameron has been mentor, colleague, laboratory oracle and confidante in equal measure. Fernando, Nora, Phil, Clarice and HeeJin have all provided invaluable support and valuable company throughout my tenure in the lab.

It would be very remiss of me to not mention my family. I would not be here without the love and guidance of my father Shri Prabhas Krishna Sinha and mother Dr. Banani Roy, and certainly would never have made it this far without the unwavering support and affection of my sister Dr. Ayesa Kaur and brother-in-law Dr. Rupinder Singh.

I would also like to thank all of the friends I have made at Cornell, who have provided a genuine camaraderie that will forever be part of my memories of Cornell.

TABLE OF CONTENTS

CHAPTER 1

INTRODUCTION

In the US, heart disease is the leading non-accidental cause of death. In 2012, it was projected that each minute someone died from a heart disease-related cause in the US. It is prevalent in all racial/ethnic groups, being the leading cause of death in African Americans, Hispanics and Caucasians and second only to cancer in Asian Americans, Pacific Islanders, Native Americans and Alaska Natives. The cost of coronary heart disease alone is estimated to cost the US $108.9 billion each year in terms of health care services, medications and lost productivity (Go, 2014).

Key factors contributing to the increase in heart disease risk are high blood pressure, high LDL cholesterol and smoking (smoking alone doubles myocardial infarction risk) (Go, 2014). Certain lifestyle choices such as excessive alcohol use, poor diet, lack of physical exercise and obesity also play a major role in increasing heart disease risk, as do medical conditions such as diabetes. With the 'baby boomer' population of the US crossing the 60-year mark, age-related risk factors are also contributing to the projected surge in heart disease cases faced by the medical community. There is an increasingly great need to understand and treat the diseases of the heart, and perhaps none more so than atherosclerosis.

Atherosclerosis (Greek: *athero* (gruel; paste) and *sclerosis* (hardness)) is a form of cardiovascular disease characterized by the thickening of an artery wall as a result of the buildup of fatty substances, cholesterol, cellular debris, calcium and fibrin in the inner lining of the artery, forming a 'plaque'. While some thickening and hardening of the arteries is a part of the

normal aging process, advanced atherosclerotic plaques can carry the risk of partially or completely blocking blood flow through the artery, resulting in strokes or heart attacks. Atherosclerotic plaques are of two types: stable and unstable. Stable plaques, generally rich in extracellular matrix (ECM) proteins and smooth muscle cells, tend to be asymptomatic. Unstable plaques, in contrast, are rich in macrophages, foam cells and cellular debris with a relatively weak but stiff fibrotic cap, which is prone to rupture (Virmani, 2002). Rupture of such unstable plaques can lead to the accumulation of the debris in the arteries, causing inappropriate clotting activity and the formation of a blood clot within the vessel, called a thrombus. Such thrombi can occlude arteries outright (coronary occlusion) or can break up and move downstream to block smaller branches of the arterial system (thromboembolism). This loss of blood flow is a major cause of heart attacks and strokes. In addition, chronic atherosclerotic lesions can cause occlusion without detaching, but remain asymptomatic until about 80% of the artery is blocked (stenosis), where downstream blood supply to tissue is so low as to cause tissue damage (Virmani, 2002). Clinically urgent atherosclerosis is most often exhibited in adults over 45 years of age, but the first signs of atherosclerosis (sub-clinical atherosclerosis) can start to appear as early as infancy or even birth (Go, 2014). Thus, atherosclerosis is a major health risk that can go undetected for a long period of time before detection and treatment. Therefore, there is an urgent need to fully understand the mechanisms that promote atherosclerotic plaque formation in order for risk determination and early detection to be effective in atherosclerosis treatment.

Atherosclerotic tissues exhibit a wide range of mechanical stiffnesses, from the pliable fatty streaks of early lesions and the necrotic core of advanced plaques, to the calcified fibrotic caps present in advanced lesions (Tracqui, 2011). Lesion progression changes the elastic environment

of the artery wall to that of a compliant core capped with a tough sheath. Since cellular function, specifically macrophage function, is affected by the mechanical properties of the environment response (Fereol, 2006; Vonna, 2007; Flannagan, 2010; Patel, 2012) and macrophages play an important role in atherosclerosis progression, there is a need to determine the effect of substrate stiffness on macrophage functions relevant to atherosclerosis. To answer this question, I utilized a 2-dimensional polyacrylamide hydrogel matrix to model atherosclerotic tissues of various stiffnesses. I plated macrophages on the gel assemblies and determined the effect of variation in substrate stiffness on three macrophage functions that are important in atherosclerosis: secretion of inflammatory cytokine, phagocytosis and lipid handling. I found that decrease in substrate stiffness increases inflammatory cytokine secretion and lipid retention while decreasing phagocytotic activity. Furthermore, I attempted to disrupt the mechanisms by which macrophages sense the mechanical properties of their environment (a process known as mechanosensing) and evaluate the resultant effect, if any, on inflammatory cytokine production. While initial results were inconclusive, there was some evidence suggesting that disruption of mechanosensing may indeed affect the inflammatory response in macrophages. This information may provide for the creation of novel atherosclerosis therapeutic strategies that target inflammation.

1.1 Atherosclerosis and Macrophages

Atherosclerotic lesions predominantly occur in arteries at sites where laminar blood flow is disturbed, such as arterial branch points and bifurcations (Moore, 2011). Studies of the earliest stages of atherosclerosis suggest that a key step is initiating accumulation of apolipoprotein B-containing lipoproteins (LPs) in the subendothelium (Williams and Tabas, 1995). The early

inflammatory response to retained apoB-LPs is activation of the overlying endothelial cells in order to recruit blood-borne monocytes (Glass and Witztum, 2001; Mestas and Ley, 2008). Monocytes are recruited by chemokines, which can be prevented by blocking the chemokines or their receptors, thus retarding atherogenesis in mouse models (Mestas and Ley, 2008). Macrophages arising from these monocytes secrete apoB-LP-binding proteoglycans (Williams and Tabas, 1995), which contribute to amplification of LP retention and subsequent failure of inflammatory resolution in atherosclerotic lesions and maintenance of inflammation. Reduction in macrophage numbers due to lack of macrophage colony-stimulating factor (M-CSF) confers protection from atherosclerosis in ApoE deficient mice in spite of hyperlipidemia (Smith, 1995; Rajavashisth, 1998). In the absence of M-CSF, monocyte-macrophages are no longer recruited to the subendothelial region and can no longer scavenge the accumulated lipid to form lipid loaded foam cells that can accumulate to form fatty streaks and eventually complex fibrous lesions. Normal macrophage presence and function is therefore necessary to control atherosclerotic plaque formation.

1.2 Macrophages and lipid handling

Monocyte differentiation into macrophages is driven by multiple factors, such as M-CSF and granulocyte-macrophage colony-stimulating factor (GM-CSF). In atherosclerotic lesions, monocytes primarily become cells that have features of macrophages and/or dendritic cells (Johnson and Newby, 2009; Paulson et al., 2010). In all stages of atherogenesis, many macrophages and dendritic cells have membrane bound lipid droplets in the cytoplasm. These lipid-loaded cells are called foam cells, and are formed when phagocytes ingest and process apoB-LPs. Once ingested, the cholesteryl esters of LPs are hydrolyzed in late endosomes to

cholesterol and fatty acids (Maxfield and Tabas, 2005). Delivery of free cholesterol to the endoplasmic reticulum normally suppresses the sterol-regulatory element binding pathway (SREBP) and downregulates endogenous cholesterol synthesis (Brown and Goldstein, 1997), which controls fat buildup in a healthy individual. Free cholesterol undergoes re-esterification to cholesteryl fatty acid esters due to the ER enzyme acyl-CoA:cholesterol ester transferase (ACAT) (Brown, 1980). Cholesterol efflux, where free cholesterol released from lysosomes and from rehydrolyzed cholesteryl ester droplets traffic to the plasma membrane and efflux out of the macrophage (Tall et al., 2008; Rothblat and Philips, 2010), is thought to be a major player in atherosclerotic plaque regression upon reversal of hypercholesterolemia. In atherosclerosis, defects in cholesterol efflux from cells or in ACAT function lead to free cholesterol-induced toxicity and may promote macrophage death in advanced atherosclerotic lesions (atheromata) (Yvan-Charvet, 2007; Zhu, 2008; Tang, 2009). Additionally, free cholesterol efflux appears to be defective in lesional macrophages, which may explain the lack of lesion regression (Jerome, 2006). Macrophages, therefore, play a central role in lipid handling and clearance and loss of these functions is an important factor in plaque formation and progression.

Numerous factors that retard plaque progression have been discovered. Research has shown that sterol-regulated transcription factors liver X receptor (LXRα and LXRβ) induce the ABC transporter proteins ABCG1 and ABCA1 and assist in regression of foam cell lesions (Calkin and Tontonoz, 2010), confirmed by targeting these genes in mice and injecting them with macrophages containing radiolabeled cholesterol, then tracking the appearance of the radiolabel in blood and feces (deGoma, 2008). ABCA1 and ABCG1 aid in cholesterol efflux from lipid-laden macrophages by translocating phospholipids and cholesterol onto nascent High Density

Lipoprotein (HDL) particles (Vedhachalam, 2007; Gillotte-Taylor, 2002, Wang, 2004, 2006). Statin drugs, which lower cholesterol levels by inhibiting the enzyme HMG-CoA reductase (which plays a central role in cholesterol production in the liver), also act by upregulating or downregulating ABC transporter expression according to cellular cholesterol abundance or scarcity respectively (Wong, 2008). As a result, therapeutic strategies to promote lesion regression include enhancing macrophage cholesterol efflux by increasing HDL (or similar particles) content or upregulating ABC transporter function (Tall et al., 2008; Rothblat and Philips, 2010).

One of the central unanswered questions in atherogenesis is how loading of macrophages with lipoprotein derived-cholesterol promotes proatherogenic activities of macrophages. Even under normal cholesterol esterification conditions, macrophages upon exposure to atherogenic lipoproteins undergo cholesterol enrichment in the plasma membrane, which may enhance inflammatory signaling through clustering-mediated activation of signaling receptors (TLR4/CD14) due to the increased order of parameter of cholesterol-enriched membranes (Yvan-Chavet et al., 2007, Zhu et al., 2008; Tang et al., 2009). Modified lipoproteins such as oxysterols and oxidized phospholipids delivered via uptake of oxidized lipoproteins can induce macrophage apoptosis. Apoptotic cells that are not cleared by macrophages via phagocytosis can eventually no longer maintain plasma membrane integrity. These cells then rupture, releasing pro-inflammatory cellular debris into the environment and thus promoting atherogenesis. Effects of lipoprotein loading were studied by gene ontology analysis of proteins differentially expressed by peritoneal macrophages from isocaloric- vs. fat-fed Low-Density Lipoprotein Receptor (*Ldlr*)-deficient mice (which have high LDL levels and develop atherosclerosis on a high-fat

diet) (Becker et al., 2010). A large number of proteins, mediated by a decrease in ApoE expression in the cholesterol-loaded macrophages and previously implicated in lesion development in gene-targeted mouse models, were found to have differential expression. Upon treatment with atherosclerosis-decreasing drugs (a statin and a thiazolidinedione), the difference in lesion development-related gene expression profiles in macrophages between the normal- and fat-fed *Ldlr*- mice decreased. Such studies have provided vital information regarding the macrophage response to protein loading *in vivo* and have also shown the applicability of systems biology approaches to atherosclerotic disease research.

1.3 Inflammatory Activation of Macrophages in Atherosclerotic Lesions

The mechanisms and effects of macrophage-mediated inflammation are an important aspect of atherosclerosis and a central focus in research. Inflammation markers were identified using immunohistochemistry and RNA analysis of laser capture micro-dissection isolated plaque macrophages from animal models and human tissues (Shibata and Glass, 2009). Several studies examining the effect of pro- or anti-inflammatory reagents and genes have revealed that factors that decrease inflammation also have a protective effect on lesion area. Selective ablation of the IκB kinase gene (involved in NF-kB activation in macrophages and neutrophils) in mice and subsequent donation of bone marrow to *Ldlr* knockout mice kept on a high fat diet resulted in an increase in atherosclerotic area in spite of a ~50% decrease in NF-kB activation and LPS-induced TNFα (Kanters et al., 2003). In contrast, endothelial-targeted inhibition of NF-kB signaling in *Apoe* knockout mice resulted in a decrease in lesion area due to a decrease in the recruitment of macrophages to lesions (Gareus, 2008). Monocyte-derived macrophages cultured from *Ldlr* knockout mice upon LPS treatment showed decreased IL-10 secretion (IL-10 being

atheroprotective in mice) (Han, 2010). Global deletion of members of the Toll-like Receptor (TLR) family (which include NF-κB in their activation pathways leading to proinflammatory cytokine production in macrophages) decrease lesion area in fat-fed *Ldlr*- or *Apoe*- deficient mice (Curtiss and Tobias, 2008). TLRs, key components of the innate immune system, elicit both protective and detrimental roles in atherosclerosis. *Ldlr*-deficient mice fed a high-fat diet and transplanted with bone marrow from *Tlr2*- deficient mice showed a decrease in lesion size only upon challenge with TLR2 agonists (Mullick et al., 2005). TLR3 deletion in *Ldlr*-knockout mice significantly reduced inflammation and atherosclerotic burden (Lundberg, 2013). TLR4 loss in *ApoE*-deficient mice reduced atherosclerosis and altered plaque phenotype (Michelsen, 2004). The TLR4/TLR6 heterodimer cooperates with CD36 in activating NF-kB in response to oxidized LDL (Stewart et al., 2010). In contrast, TLR7 plays an atheroprotective role by interfering with the proinflammatory responses to TLR2 and TLR4 ligands, as functional inactivation of TLR7 in ApoE-deficient mice led to accelerated lesion development and increased plaque vulnerability (Salagianni, 2012). Fat-fed *Ldlr*- knockout mice transplanted with bone marrow from *Cd40*-knockout mice also showed a reduction in lesion area and inflammation (CD40 being a macrophage receptor with the capability to trigger NF-kB activation) (Lutgens et al., 2010). Exposing macrophages to cholesterol crystals, present in atherosclerotic plaques from early on, induces inflammation via an inflammasome complex comprised of multiple proteins such as NLRP3, ASC and caspase-1. In *Ldlr*- knockout mice fed a fat-rich diet, transplantation with marrow cells lacking NLRP3 or ASC resulted in a decrease in lesion size and levels of the proinflammatory cytokine IL-18 (Duewell, 2010; Rajamaki, 2010). Thus, multiple inflammation factors have been identified as playing a role in lesion formation, providing opportunities to

develop novel therapeutic strategies that target inflammation pathways in order to cause lesion regression or prevention.

1.4 Defective Efferocytosis in Atherosclerotic Lesions

The greatest health risk posed by advanced atherosclerotic plaques is the risk of plaque rupture, which can lead to thrombosis (blockage of the vessel lumen) and release of the toxic products of cell necrosis (toxic enzymes, oxidants, proteases, caspases etc.) from the necrotic core. Necrotic cores arise from the combination of apopotosis of advanced lesional macrophages and defective phagocytotic clearance (efferocytosis) of the apoptotic cells in advanced plaques (Tabas, 2010). In early lesions the efferocytic clearance is efficient enough to cause decreases in lesion cellularity, inflammation and plaque progression rather than an increase in plaque necrosis. At that stage, macrophages are able to clear cells before membrane damage leads to extracellular leakage of toxic intracellular material. This triggers an IL-10 and TGF-β –mediated anti-inflammatory response in the efferocytes and promotes efferocyte survival by protecting them from potentially toxic factors present in the apoptotic cells. Macrophage death in advanced lesions can be due to any of a number of processes – growth factor deprivation, oxidative stress and/or death receptor activation (Tabas, 2010).

Excess apoB-LP buildup in the subendothelial space causes endothelial and smooth muscle cell toxicity and death, the products of which would normally be cleared by efferocytosis. Once efferocytic clearance is unable to sufficiently clear the apoptotic cells, the apoptotic cells build up, causing secondary necrosis and release of inflammatory cellular contents into the subendothelial space. Normal efferocytic clearance involves robust esterification and efflux of cholesterol, efflux of proapoptotic oxidized lipids, and activation of Akt and NF-kB cell survival

pathways. Efferocytosis is carried out via phagocytotic receptors such as tyrosine kinase MerTK, low-density lipoprotein receptor-related protein 1 (LRP-1), apoptotic cell ligands such as phosphatidylserine and C1q and bridging molecules such as Growth arrest-specific 6 that recognize apoptotic cells (Henson et al., 2001). Since efferocytosis is a high-capacity process and its throughput is unaffected by artificially increased apoptotic rates (via genetic manipulation in early atherosclerotic lesions) (Tabas, 2010), the combination of overabundant apoptotic macrophages and widespread tissue necrosis causing plaque necrosis would imply that the process of efferocytosis itself becomes defective in advanced atherosclerotic lesions. There are multiple possible explanations for this loss of function, such as oxidative stress-induced macrophage death due to defective cholesterol efflux after apoptotic cell engulfment (Yvan-Charvet et al., 2010); LP-associated hydrolysis of oxidized phosphatidylserine on apoptotic cell surfaces by phospholipase A2 (Wilensky and Macphee, 2009); and/or protease-mediated cleavage of the efferocytosis receptor MerTK (Sather et al., 2007). Since atherosclerosis and obesity are two highly-correlated health risks, there is also the potential explanation of defective engulfment of apoptotic cells by macrophages that have been exposed *in vivo* or *in vitro* to saturated fatty acids, possibly due to changes in plasma membrane structure (Li et al., 2009).

1.5 Mechanosensing and Atherosclerosis.

While cytokine and chemokine cues are critical ways to influence cell fate and function, several recent studies provide evidence that cells sense and respond to their physical environment in a process known as mechanosensing. Naïve mesenchymal stem cells (MSCs) can be committed to specific lineage and phenotypes by altering the stiffness of the growth substrate, even when cultured in the same mix of growth and differentiation factors. MSCs grown on softer substrates

mimicking nervous tissue had neuron-like RNA expression profiles and had osteocyte-like RNA expression on stiffer substrates mimicking bone (Engler, 2006). This matrix stiffness-dependent lineage commitment of MSCs is mediated by the α_2-integrin subunit of the $\alpha_2\beta_1$ integrin, via intracellular signaling through the mechanotransducers Rho kinase (ROCK) and focal adhesion kinase (FAK) (Shih, 2011). ROCKs are downstream targets of the small GTP-binding protein RhoA. ROCKs are characterized for their roles in mediating the formation of RhoA-induced stress fibers and focal adhesions, changing the actin cytoskeletal structure through effects on myosin light chain phosphorylation (Leung, 1996; Somlyo, 2000). Matrix stiffness thus has a role in stem cell fate determination, driven by mechanotransducer kinase-driven mechanosensing events.

Effects of substrate mechanical stiffness are not limited to undifferentiated cells alone. Endothelial cells cultured on hydrogels mimicking the elasticity of young or aging arterial inner walls (intima) show increased permeability and disrupted cell-cell junctions on stiffer matrices (aged intima) (Huynh, 2011). This destabilization of cell-cell junctions was due to increased contractility of endothelial cells on stiffer substrates. The increased permeability of the endothelium results in increased monocyte extravasation, leading to accumulation in the subendothelial region and triggering atherogenesis. Endothelial integrity was restored by inhibiting ROCK via the chemical inhibitor Y-27632 or via small interfering RNA.
The ability of culture substrates to affect cell adhesion and focal adhesion rates has been documented in macrophages (Van Goethem, 2010) as well as non-macrophage cells (kidney epithelial and 3T3 fibroblast cells, Pelham 1997), but recent studies have shown that the mechanical stiffness of substrates also dynamically affect macrophage elasticity (Fereol, 2006;

Vonna, 2007; Flannagan, 2010; Patel, 2012) and by extension, could also affect macrophage functions such as phagocytosis and inflammatory response.

Mechanical stiffness studies have found that the fatty streaks in early plaque and the necrotic core of advanced plaques have a Young's modulus of stiffness of 5-9 kPa, while the calcified hypocellular fibrotic regions of advanced plaques have a much higher Young's modulus of ~100kPa (Tracqui, 2011). Given the considerable heterogeneity in both mechanical properties and macrophage populations (atherogenic, inflammatory macrophages and atheroprotective, anti-inflammatory macrophages) (Stoger, 2010), there is reason to investigate the hypothesis that the variations in substrate mechanical stiffness within atherosclerotic lesions affect monocyte-to-macrophage differentiation and atherogenic progression biases macrophage function to be pro-inflammatory and atherogenic.

1.6 Outline of Thesis Research

Macrophage cells play a very important role in determining the fate of an atherosclerotic lesion, since loss of their abilities to clear lipid loads and efferocytose apoptotic cells is a major factor in lesion progression to advanced plaque stages. Based on the studies discussed above, we hypothesized that substrate stiffness plays an important role in regulating the ability of macrophages to clear lipid loads and apoptotic cells in atherosclerotic lesions. Based on previous research on mimicking matrix elasticities (Pelham, 1997; Huynh, 2011), we devised a means to study the effect of substrate stiffness on macrophages, by plating them on thin polyacrylamide gels laid on glass coverslips. By tuning the ratio of acrylamide to bis-acrylamide in the gel, we were able to fabricate gels of various stiffnesses (Young's modulus of 1kPa – 100 kPa). Once plated across differing substrate stiffnesses, we evaluated the plated macrophages for variations

in morphology, immune/inflammatory response to stimulation with TLR agonists (cytokine production), lipid handling and clearance, phagocytotic efficiency, the effect of inhibition of rho kinases (involved in mechanosensing) on cell morphology and reaction to TLR agonists and the effect of inhibition of actin cytoskeleton polymerization and reorganization on reactivity to TLR agonists.

There were several major findings from my thesis work. Cells plated on more compliant (softer) substrates adopted a spherical shape with lower numbers of focal adhesion bodies than those plated on stiffer substrates. Cells on softer substrates produced more proinflammatory cytokine (TNF-α) upon stimulation and had increased lipid uptake and retention but lower phagocytotic activity. Inhibition of rho kinases and actin polymerization immediately prior to stimulation of proinflammatory cytokine production did not alter TNF-α production. Loss of mechanosensing in macrophages due to rho kinase inhibition resulted in formation of new actin projections and focal adhesion bodies to resume mechanosensing, the frequency of which increased with increase in substrate stiffness. Rho kinase phosphorylation was found to be increased in cells plated on stiffer substrates, showing that rho kinases play a role in mechanosensing in macrophages.

CHAPTER 2

MATERIALS AND METHODS

2.1 Cell Culture

RAW 264.7 cells (ATCC #TIB-71) cells were cultured in Dulbecco's modified Eagle's medium (DMEM) with 2mM L-glutamine, 50 U/ml penicillin, 50ug/ml streptomycin, 10mM HEPES, 1mM sodium pyruvate and 10% low endotoxin FBS. Cells were cultured from thawed passage tested negative for mycoplasma prior to freezing.

Bone marrow cells were flushed from the femur of a C57BL/6 mouse and cultured in bone marrow-derived macrophage (BMM) media (DMEM supplemented with 2mM L-glutamine, 50 U/ml penicillin, 50ug/ml streptomycin, 10% supernatant from L929 cells, and 10% low endotoxin FBS) for five days (three passages, passing at 1:2 cells: media) before use.

2.2 Reagents

22x22 mm No. 1 Ground coverslips, 2% Bis-acrylamide and 40% acrylamide were from Fisher Scientific. 50% w/v Glutaraldehyde, 50% Polyethyleneimine (PEI), Oleic Acid, Rho kinase (ROCK1/2) inhibitor Y-27632 and Mouse anti-Vinculin antibody were from Sigma-Aldrich. Sulfo-SANPAH was from Thermo Scientific Pierce. Zymosan A (*S. cerevisiae*) BioParticles – Alexa Fluor 594 conjugate, Alexa Fluor 488 Phalloidin and Alexa Fluor goat anti-mouse 647 antibody were from Life Technologies. Bovine Serum Albumin Fraction V (heat shock, fatty acid free) was from Roche. BODIPY 493/505 dye was from Invitrogen. Lipopolysaccharide (LPS) was from Invivogen. Jasplakinolide was from Santa Cruz Biotech. Rabbit anti-phospho-

ROCK1 (Thr455/Ser456) antibody was from BioSS USA. Rabbit anti-ROCK1 antibody was from Cell Signaling. Mouse anti- α tubulin antibody was from eBiosciences. Goat anti-mouse HRP-conjugated antibody and Goat anti-rabbit HRP-conjugated antibody was from Southern Biotech. CpG DNA 10104 5' – TCGTCGTTTCGTCGTTTTGTCGTT – 3' oligonucleotides were from Integrated DNA Technologies.

2.3 Preparation of Polyacrylamide Gel-coated Coverslips and Cell Seeding

22x22 mm No.1 glass coverslips were activated by sequential coating with 1% polyethyleneimine (PEI) and 50% glutaraldehyde. After rinsing with sterile 1x PBS, coverslips were coated with polyacrylamide gels of the following stiffnesses - 1, 5, 20 or 100kPa (ratios provided in table 1).

The gel layers were created (**Figure 1**) by sandwiching the PAA mixture between an activated coverslip and a Rain-X coated (hydrophobic) coverslip and exposing the resultant assembly to vacuum for 30-60 min (vacuum treatment time was increased for more compliant gel assemblies, i.e., 1 and 5kPa gels). After the gel layer had polymerized, the top hydrophobic coverslip was removed, the gel was coated with 0.2mg/ml Sulfo-SANPAH and exposed to 305nm UV light for 10 min. Sulfo-SANPAH was washed off with 50mM HEPES.

Gels were coated with 20ug/ml fibronectin by inverting the coverslips gel-side down in a 200ul bubble of 10µg/ml fibronectin overnight at 4^{o}C. The fibronectin acted as a biological agent to assist in cellular adhesion. Each coverslip was seeded with $1x10^{5}$ RAW cells and incubated in a 6-well plate at 37^{0}C overnight before use.

Table 1: Reagent ratios to make polyacrylamide gels of given stiffness (Young's Modulus, kPa). Adapted from protocol provided by Prof. Cynthia Reinhart-King, Cornell University (Huynh, 2011).

Young's Modulus (kPa)	Volume Acrylamide (mL)	Volume Bis-acrylamide (mL)	HEPES pH6 (mL)	TEMED (µL)	MilliQ water (mL)
1.0	1.50	1.00	2.6	10	13.39
5.0	3.75	1.75	2.6	10	10.39
20	6.00	1.90	2.6	10	7.99
100	6.00	9.69	2.6	10	0

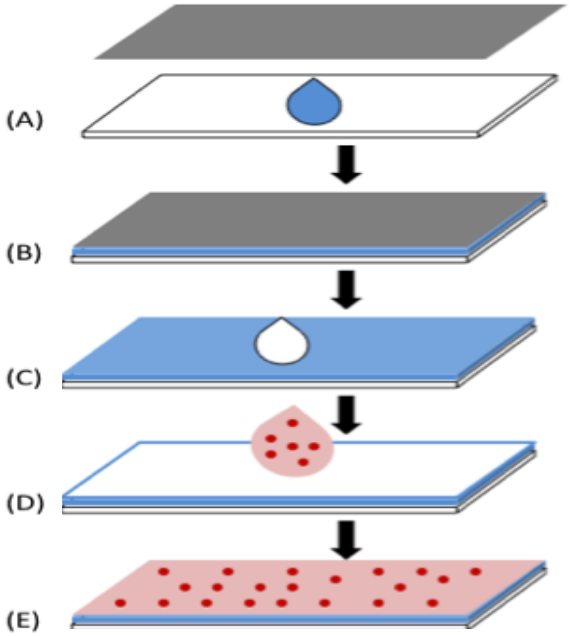

Figure 1: Schematic for generation of synthetic substrates on glass coverslips (A-B) Polyacrylamide gel of desired stiffness (blue) is coated on coverslips (white) and sandwiched with a top coverslip treated with hydrophobic product to promote even polymerization (grey). (C) The top coverslip is then removed and the gel surface cross-linked with protein (white) to facilitate macrophage adhesion. (D) Macrophages in culture media (pink) are added to the gel and allowed to settle (E) before fixation and staining.

2.4 Phagocytotic Uptake of Fluorescent Bioparticles:

RAW cells were plated at $2x10^5$ cells/coverslip on 1, 5 and 20kPa gels or glass and incubated for overnight at 37^0C. The next day, fluorescently conjugated zymosan bioparticles were added to each coverslip at a count of $2x10^6$/well (Multiplicity of Infection, MOI = 1:10). Coverslips were then incubated at 37^0C for 30 min. Post-incubation, non-absorbed particles were quenched by adding trypan blue (1.2µg/ml) and washing coverslips in PBS. Cells were fixed in 3% formaldehyde for 20 min, washed in 1x PBS and permeabilized in 0.1% Triton X-100 in PBS for 5 minutes. After washing 3x in PBS, coverslips were blocked in 1% BSA in PBS for 20 minutes. Cells were then stained with phalloidin diluted 1:40 in 1% BSA in PBS for 20 min. Coverslips were then washed 3x in PBS and air-dried before mounting on slides using ProLong Gold + DAPI mountant.

2.5 Foamy Macrophage Induction

RAW cells plated at $2x10^5$ cells/coverslip on 1, 5 and 20kPa gels and glass and were incubated overnight. The next day, oleic acid conjugated 8:1 to de-fatted BSA in 0.1M Tris-Cl (pH 8.0) (84mg oleic acid added to 3.36g BSA in 24ml 0.1M tris-Cl, vortexed and filter sterilized) was added to cells at a final concentration of 400uM oleate in DMEM. Coverslips with cells were subsequently collected at intervals of 2, 6 and 24 hours post-addition of oleate and fixed in 3% PFA for 10 min at RT before staining with BODIPY 493/505 (dissolved to 1ug/ml concentration in 150mM NaCl) for 10 min. Coverslips were then washed 3x in PBS before air-drying and mounting with ProLong anti-fade Gold with DAPI (Invitrogen/Molecular Probes).

2.6 Rho kinase/ Actin polymerization Inhibition

RAW cells plated at $1x10^5$ cells / coverslip on 1, 5, 20 and 100kPa gels and glass were incubated overnight. The next day, Rho kinase inhibitor Y-27632 [(1R, 4r)-4-((R)-1-aminoethyl)-N-(pyridin-4-yl) cyclohexanecarboxamide] was added to the cells at a concentration of 10μM for the rho kinase inhibition assay. For the actin polymerization inhibition assay, actin polymerization inducer Jasplakinolide (dissolved in DMSO) was added to the cells at a concentration of 0.5uM. An additional vehicle-only control was included by adding an equivalent volume of DMSO. Thirty minutes after addition of inhibitors, cytokine production in RAW cells was stimulated by the addition of either the TLR4 ligand bacterial lipopolysaccharide LPS (100ng/ml) or the TLR9 ligand CpG DNA (3uM). The cells were stimulated for 6 hours (Y-27632) or 9 hours (Jasplakinolide) at 37^0C before cytokine-containing supernatant was collected for analysis via TNF-ELISA. After supernatants had been collected, cells were fixed, permeabilized and stained to determine their cytoskeletal structure (staining for actin, vinculin and tubulin).

2.7 Cytokine ELISA

TNF-α production was determined using the mouse TNF-α ELISA MAX Set (BioLegend, San Diego, CA, USA) from supernatants of cells cultured with TLR ligands for 6-9 hours. Supernatants were spun down at 1400 rpm for 5 min at 4^oC for 5 minutes to remove residual cells before storage at -80^oC until use. Supernatants obtained from unstimulated cells were diluted 1:1 in assay diluent (1% BSA in PBS), while supernatants from cells stimulated with CpG DNA or LPS were diluted 1:10 in assay diluent for use in assay. Means and standard

deviations of sample data were calculated in Microsoft Excel 2010 and data analyzed and graphed in GraphPad Prism.

2.8 Staining of Cells for Cytoskeletal Elements

Cells were fixed in 3% paraformaldehyde and subsequently permeabilized with 0.1% Triton X-100 before blocking in 1% BSA for 1 hr. Afterwards, cells were stained with primary antibodies against Vinculin (Sigma-Aldrich V9131 mouse anti-vinculin) or Tubulin (eBiosciences mouse anti-α tubulin 14-4502) (both at concentrations of 1:400 in 1% BSA in PBS) where indicated. Secondary staining was performed with Life Technologies Goat anti-mouse Alexa Fluor 647 antibody (common to both anti-vinculin and anti-tubulin antibodies) at a concentration of 1:400. Staining with Life Technologies Alexa Fluor 488-phalloidin (1:200) was done in parallel. Coverslips were mounted using Life Technologies Prolong anti-fade Gold with DAPI. Coverslips were imaged via confocal microscopy on the Leica TCS SP5 microscope system and images stored in individual channels in TIFF format. Composite images were assembled in Adobe Photoshop. Quantitative data (cell number, size, cytoskeletal projection length) were obtained with the assistance of micron scale generated alongside images and averaged over multiple fields, slides and experiments per experimental condition. Data was analyzed in GraphPad Prism.

2.9 Protein Immunoblotting Assay (Rho kinase Phosphorylation)

RAW 264.7 cells were lysed in Laemmli reduced sample buffer (1% SDS, 12.5% Glycerol, 0.005% bromophenol blue, 62.5 mM Tris pH 6.8, 1.7% beta-mercaptoethanol) by inverting coverslips (plated with cells) over 100ul lysis buffer bubbles for 1-2 minutes before collection in

1.5ml microcentrifuge tubes. Samples were boiled at 95^{o}C for 5 min prior to storage at -80^{o}C. For analysis, samples were again boiled, sonicated using probe sonication (10seconds/sample) and resolved on 0.8% SDS PAGE gels. Proteins were then transferred (15V, 37 min in a Bio-Rad Trans-Blot SD semi-dry transfer cell) to nitrocellulose membranes, and immunoblotted for ROCK1, phospho-ROCK1 or tubulin. The nitrocellulose membranes were blocked in TBST (Tris-buffered saline + 0.1% Tween-20) + 5% w/v BSA for 1 hour for the ROCK1 and phospho-ROCK1 immunoblots and in TBST (Tris-buffered saline + 0.1% Tween-20) + 5% w/v nonfat dry milk overnight at 4^{o}C for the tubulin immunoblot. After blocking, membrane was immersed in a solution of anti-ROCK1 mAb (Cell Signaling C8F7, Rabbit) or anti-phospho-ROCK1 Ab (BioSS bs-4063R, Rabbit) diluted 1:1000 in TBST + 5% w/v BSA (for ROCK1 and phospho-ROCK1 respectively) overnight at 4^{o}C with gentle rocking. The tubulin immunoblot was rocked in a solution of anti-alpha-tubulin Ab (eBiosciences 14-4502, mouse) diluted 1:1000 in TBST + 1:20 blocking solution for 1 hour at room temperature. Membranes were then washed 3x 5min in TBST and incubated in secondary antibody (Goat anti-Rabbit HRP, Southern Biotech for ROCK1 and phospho-ROCK1 and Goat anti-Rabbit HRP, Southern Biotech for tubulin) diluted 1:10,000 in TBST for 1 hour. After secondary antibody incubation, membranes were washed 3x 5min in TBST and developed with Thermo Scientific Super Signal West Pico chemiluminescent reagent. X-ray film was used to determine presence of desired proteins (ROCK1/phospho-ROCK1/tubulin). Densitometric analysis of protein bands to determine protein amounts was done in ImageJ. Quantitative data was plotted in Prism.

CHAPTER 3

RESULTS

3.1 Changes in substrate stiffness alter macrophage morphology and cytokine production.

Macrophages are able to sense the stiffness of their surroundings via mechanosensing. In order to determine the effect of substrate stiffness on macrophage morphology, specifically in the distribution of the actin filaments of the cytoskeleton, I plated primary murine bone marrow-derived macrophages on 20kPa gels on 22x22mm glass coverslips or glass coverslips alone and visualized their actin cytoskeletal structure by staining the plated cells with Alexa 488-conjugated phalloidin and subsequently imaging them via fluorescent microscopy. On the 20kPa gel, macrophages adopted a small footprint and bright green actin rings, regions of high actin density (**Figure 2, right**). In contrast, on glass, cells were spread out over a large area and exhibited two-dimensional actin meshes called lamellipodia. The actin rings were replaced by irregular patches of high actin density in cells plated on glass (shown in inset box, **Figure 2, left**). The morphological characteristics of the cells are summarized in **Table 2**. These findings are consistent with a previous study performed with alveolar macrophages (Fereol, 2006).

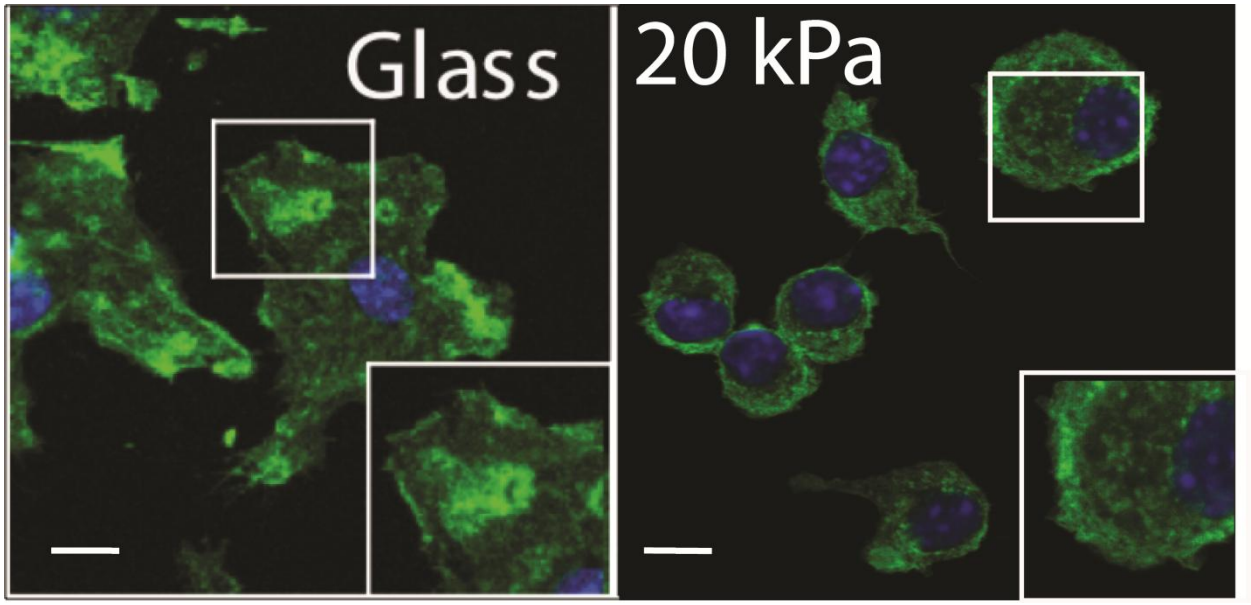

Figure 2: Macrophage morphology changes across substrates with different modulus of elasticity. Primary mouse macrophages were plated overnight on glass or 20kPa gels. After fixation and permeabilization, cells were stained with phalloidin-Alexa 488 (Green, showing actin cytoskeleton) and mounted using ProLong AntiFade Gold with DAPI (Blue, staining double-stranded DNA and denoting the nucleus). Scale bars = 10 μm. Inset boxes in the bottom right corner of each field are 2x magnification views of the regions enclosed in the white square of the respective image). Images were acquired on a Leica SP5 confocal microscope and compiled in Photoshop. Images are representative of 5 independent experiments.

Table 2: Characterization of primary bone marrow macrophages plated on 20kPa gels or glass. Numbers are representative of 50 cells imaged across four fields per slide, two slides per experimental condition over 5 independent experiments.

Substrate type	Average Nucleus size (μm)	Average Cell size (μm)	Actin ring?	Number of Actin projections/cell, type
20kPa	10	20	yes	15.22±0.33, filopodia
Glass	10	30	No	35.14±0.97 filopodia, lamellipodia

Atherosclerotic plaques contain regions of various stiffnesses, and contain macrophage populations that have different inflammatory profiles. To determine whether the variations in mechanical stiffness within atherosclerotic plaque affects macrophage inflammatory profiles, the amount of proinflammatory cytokine produced by macrophages was measured in supernatants of cells plated on rigid and elastic surfaces. Primary bone marrow-derived macrophages were plated on 20 kPa gels or on glass (50 gPa) coated with BSA or poly-l-lysine (PLL) and then stimulated with media alone or CpG DNA 10104 (3 μM). CpG DNA oligonucleotides are a common motif in prokaryotic DNA and are a potent inducer of macrophage activation and subsequent proinflammatory cytokine production (Ramirez-Ortiz, 2008). Cells plated on 20kPa gels had higher basal levels of TNF-α secretion than those plated on glass (**Figure 3A**), and the TNF-α secretion in response to stimulation with CpG DNA was higher for cells plated on 20kPa gels vs. glass as well. The TNF-α response in cells on the compliant gel substrate was independent of biomatrix chemistry, being higher irrespective of whether the substrates were coated with BSA or PLL. Calculation of the fold induction revealed that cells plated on the 20kPa gel had a smaller increase in TNF-α secretion than cells plated on glass when stimulated with CpG DNA (**Figure 3B**). Together, these data suggest that substrate stiffness affects both macrophage morphology and inflammatory response, but further studies will be required which would include normalizing the response for cell numbers via qPCR analysis. Increased background seen in cells on gel may be due to altered sensitivity to stimuli, which may be studied by evaluating a CpG DNA dose response.

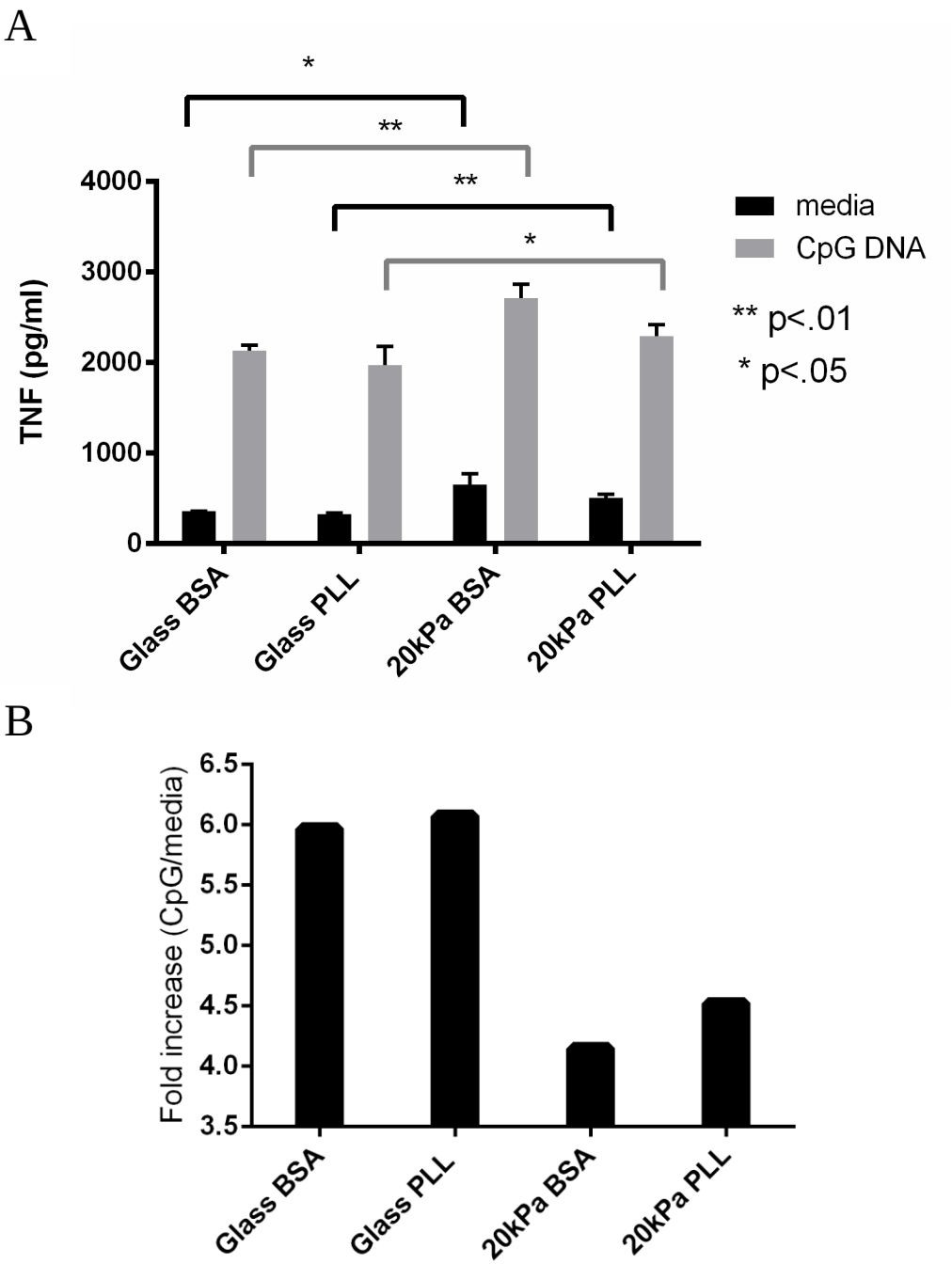

Figure 3: Proinflammatory cytokine production in macrophages increases with increase in substrate stiffness. (**A**) Primary bone marrow-derived macrophages were plated on 20kPa polyacrylamide gel or glass (50gPa), coated with either BSA or PLL as the biologic surface agent and stimulated with media or CpG DNA oligonucleotides. Supernatants were collected after 6 hours of stimulation and TNF-α was quantitated via ELISA (commercial kit). (**B**) Fold increase in TNF response of cells. Representative of three independent experiments. **: $p<0.01$, *: $p<0.05$, unpaired t-test.

3.2 Increase in substrate stiffness promotes macrophage phagocytotic activity

Phagocytosis is the key defining function of macrophages. We next determined whether the changes in macrophage morphology and proinflammatory cytokine production were accompanied by changes in the cells' ability to perform phagocytosis. Primary bone marrow-derived macrophages plated on gels of varying stiffnesses were incubated with *Saccharomyces cerevisiae* zymosan bioparticles. Fluorescent imaging (**Figure 4A)** revealed that the macrophages plated on more compliant gels had a lower phagocytotic capacity. Macrophages plated on 20 kPa gels had a higher percentage of cells that phagocytosed bioparticles than those plated on 5 kPa gels (**Figure 4B**). Cells plated on glass phagocytosed 9±2.2 particles/cell, whereas cells plated on 5kPa and 20kPa gels engulfed 1.35±0.9 and 2.5±1.14 zymosan particles/cell respectively (**Figure 4C**). This demonstrates that substrate stiffness also affects macrophage phagocytosis.

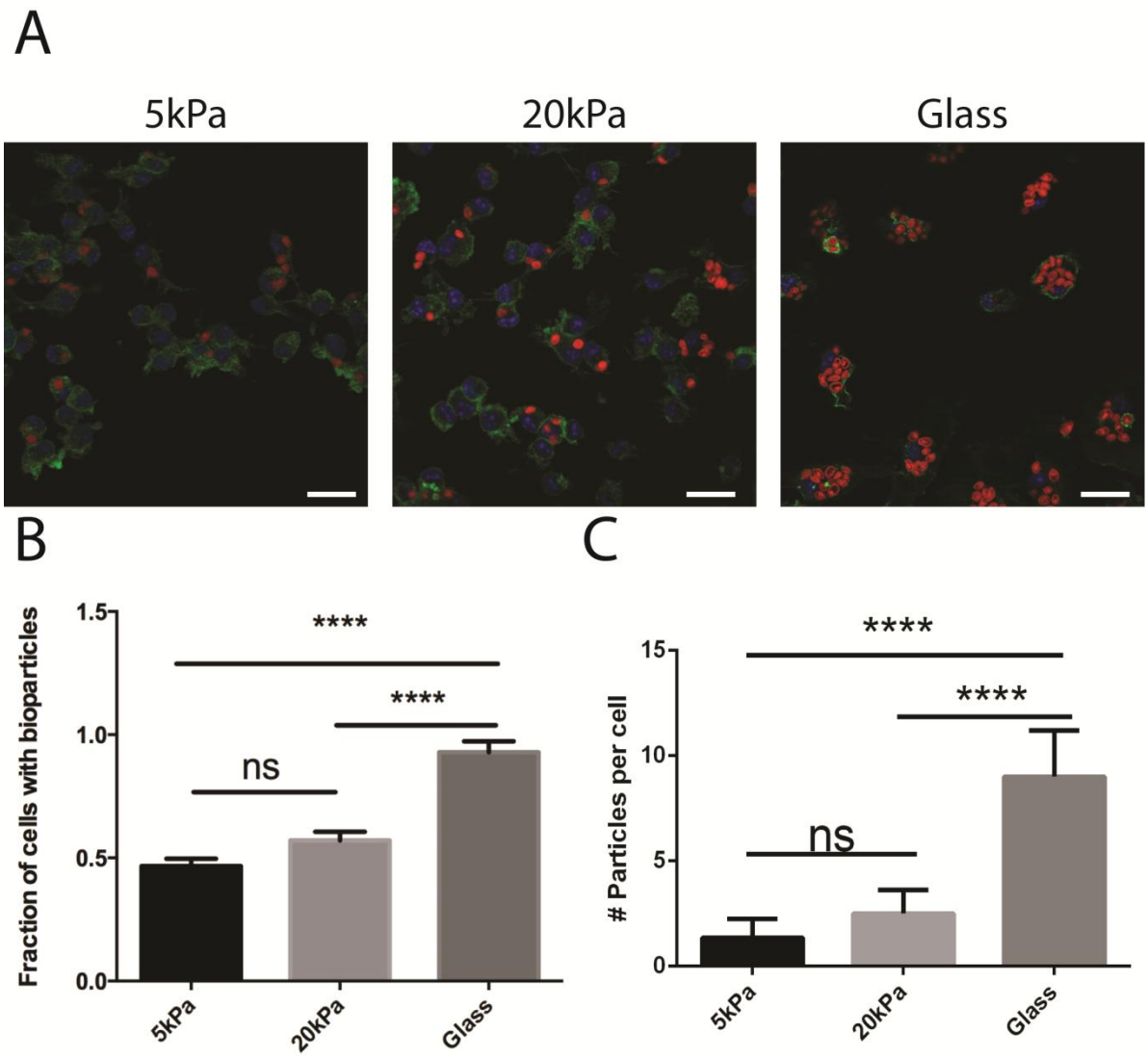

Figure 4: Increase in substrate rigidity leads to increase in bioparticle phagocytosis. (A) Primary murine bone marrow-derived macrophages plated on either glass coverslips or 5kPa or 20kPa PAA gels on coverslips were exposed to Life Technologies Alexa Fluor 594-conjugated Zymosan A (*Saccharomyces cerevisiae*) particles (red) and stained with Alexa Flour 488-phalloidin (actin cytoskeleton, green) and DAPI (nuclei, blue). Images were acquired on a Leica SP5 confocal microscope at 40x magnification, complied in Photoshop and are representative of three independent experiments. **(B)** Fraction of total number of cells that have phagocytosed bioparticles. **(C)** Average # of bioparticles per cell, each cell having phagocytosed minimum one bioparticle. Numbers are calculated from an average of ~100 cells measured across two fields per slide, two slides per experiment over three independent experiments. Statistical significance determined in GraphPad Prism via one-way ANOVA with alpha = 5%. **** = $P \leq 0.0001$, ns = $P > 0.05$. Scale bars = 20 µm.

3.3 Lipid uptake and clearance rates are affected by substrate stiffness

Lipid handling and clearance is one of the primary tasks of macrophages in regulation of atherosclerosis. Therefore, we next evaluated lipid uptake and clearance by macrophages plated on substrates of varying stiffness. Oleate was added to primary bone marrow-derived macrophages plated on 5 kPa or 20 kPa gels or glass, coated with 0.1% w/v BSA at a final concentration of 400 μM, and the cells were collected after 2, 6 or 24 hours (**Figure 5E**). Lipid uptake was observed as early as two hours in cells grown on more compliant gels (5kPa), but lipid droplets were not observed until later on stiffer gels (20kPa) or glass (**Figure 5A**). Cells grown on 5kPa gels retained a larger number of lipid droplets than those plated on glass after 24 hours (**Figure 5B**). Furthermore, more lipid droplets were observed per cell when cells were grown on compliant gels (**Figure 5C**). Although the number of droplets was less at 24 hours than at 6 hours for cells grown on 5kPa gels, many of the droplets appeared larger in size (**Figure 5B, 5D**). These results indicate that lipid uptake and retention is increased in macrophages plated on more compliant substrates.

Figure 5: Increased substance stiffness leads to lower lipid retention. Primary murine bone marrow macrophages were exposed to oleate and were collected at the following timepoints: 0 hours (before addition of oleate), 2 hours, 6 hours and 24 hours. Cells were stained for lipid using BODIPY 493/505 dye (Green) and nuclei with DAPI (blue). Coverslips were imaged on a Leica SP5 confocal microscope. White arrows point to lipid droplets. Images are representative of three independent experiments. (**A**) Green-stained lipid droplets were visible on 5kPa gels after 2 hours but not on glass. **(B)** Lipid droplets were still present in cells on 5kPa gels after 24 hours but not on glass. (**C**)Statistical analysis of lipid droplets in cells, showing average number of lipid droplets per cell, across 5kPa, 20kPa and glass over four collection times. **(D)** Average number of small (<1 um dia.) and large (>1um dia.) lipid droplets per cell, across 5kPa and 20kPa gels and glass, over time, showing relative rates of clearance of smaller lipid droplets versus larger volumes in cells plated on substrates of varying stiffness. Data represents an average of ~200 cells imaged across two slides per stiffness per experiment, over three experiments. Statistical significance was determined in GraphPad Prism via 2-way ANOVA using the Tukey method, with alpha = 5%. **** = $P \leq 0.0001$, ns = $P > 0.05$ (**E**) Representative images of cells plated on the three substrate types and imaged at each of the 4 collection timepoints.

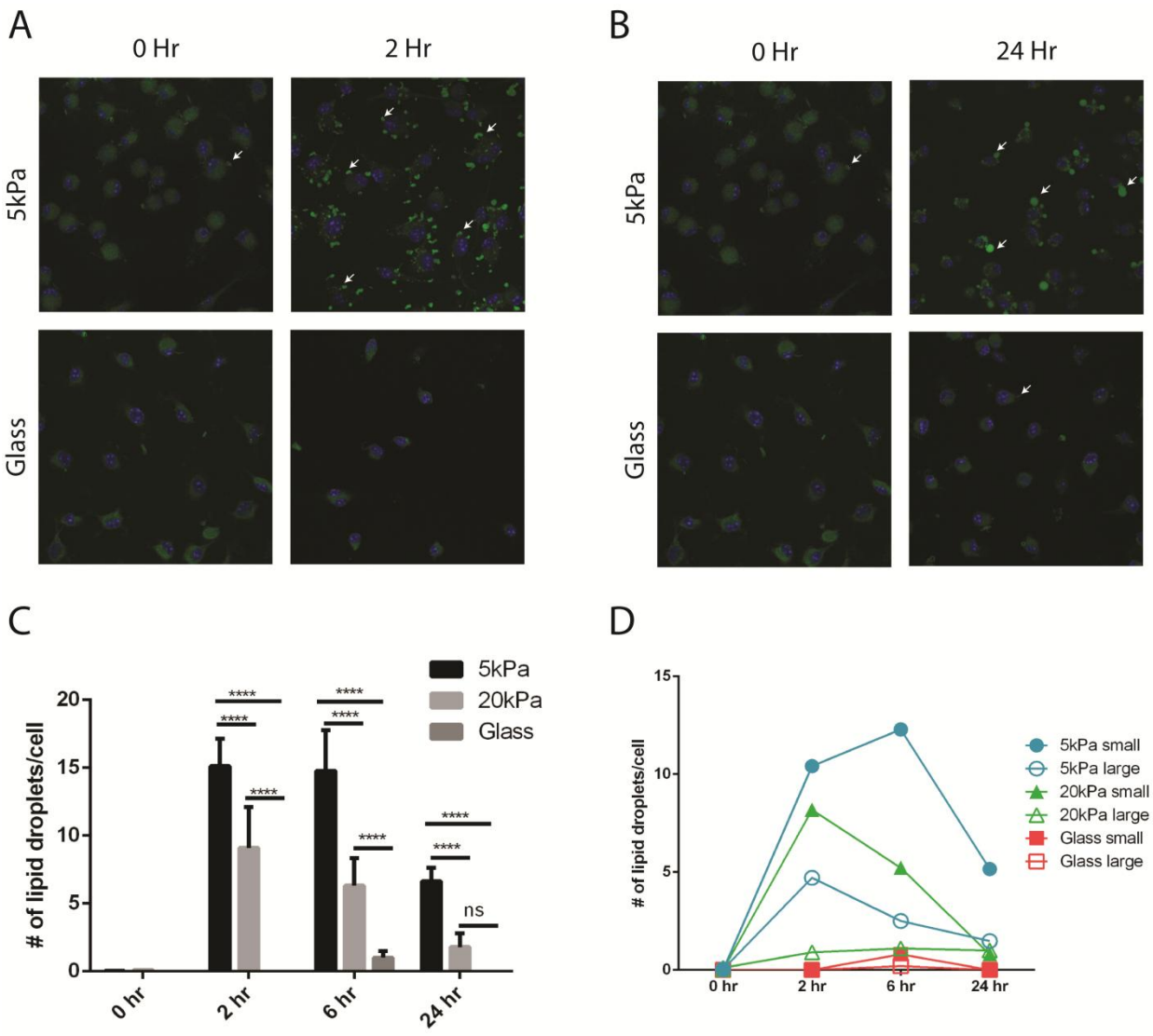
A
0 Hr
2 Hr
5kPa
Glass
B
0 Hr
24 Hr
5kPa
Glass
C
5kPa
20kPa
Glass
# of lipid droplets/cell
20
15
10
5
0
****
****
****
****
****
****
****
ns
0 hr
2 hr
6 hr
24 hr
D
# of lipid droplets/cell
15
10
5
0
0 hr
2 hr
6 hr
24 hr
5kPa small
5kPa large
20kPa small
20kPa large
Glass small
Glass large

Figure 5 (Continued)

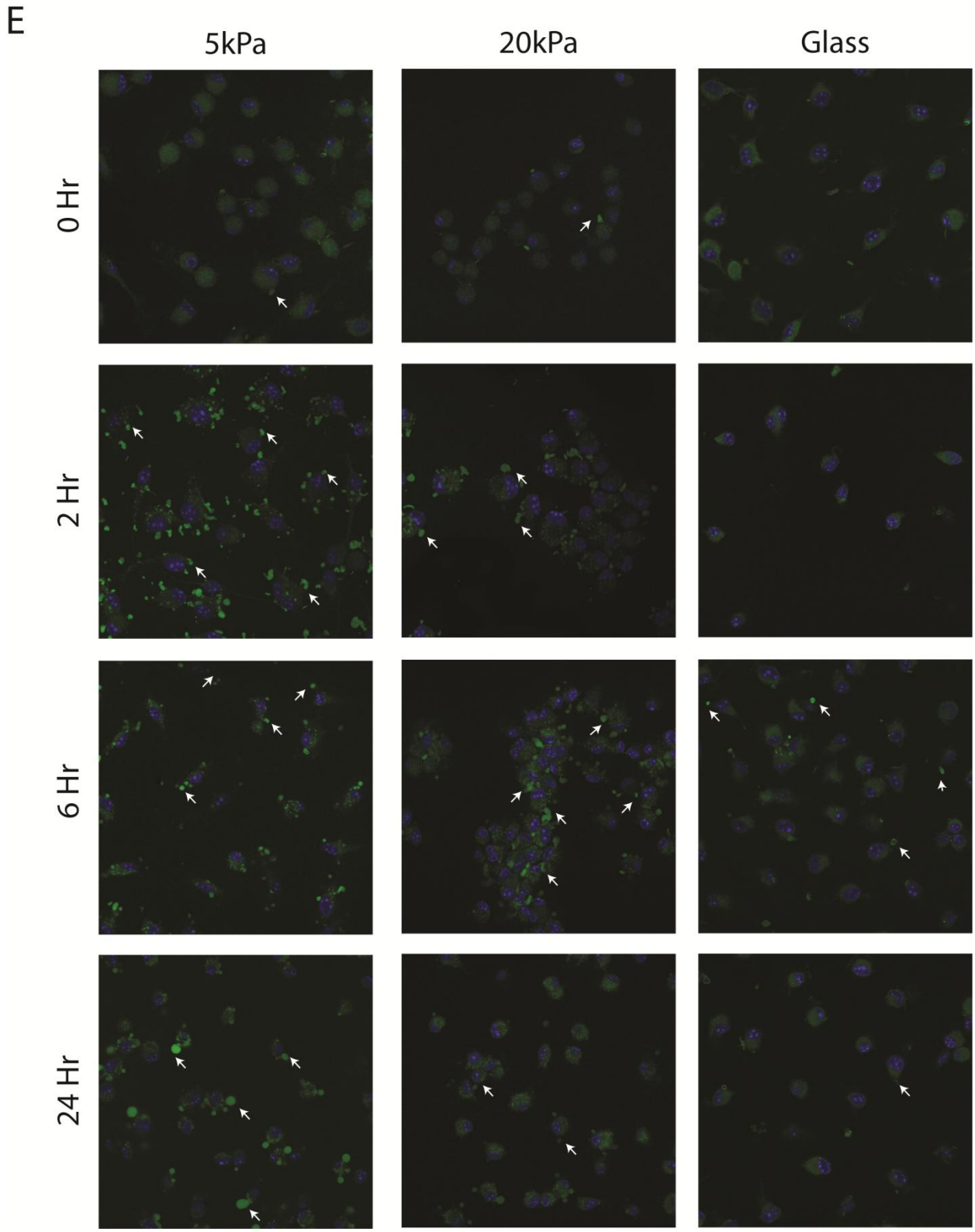

3.4 Rho kinase inhibitor affects cell morphology and TNF-α production in activated macrophages.

Rho kinases (ROCK) are known to mediate mechanosensing pathways and have been found to play a critical role in cardiovascular disease (Loirand, 2006; Shimokawa, 2007, Zhou, 2011). To determine whether ROCK participated in mechanosensing and the inflammatory response, we next evaluated the effect of ROCK inhibitors on macrophage morphology and TNF-□ production. RAW264.7 macrophages were pretreated with a rho kinase inhibitor Y-27632 that blocks the activity of both ROCK1 and ROCK2 (Uehata, 1997), and stimulated with CpG DNA or LPS. Cytoskeletal components actin, tubulin and vinculin were resolved for imaging via fluorescent staining. On softer matrices (1 and 5 kPa - **Figure 6B, 6C**), the RAW cells adopted a small circular footprint, as visualized by a prominent but thin actin 'ring' around the nucleus whereas on stiffer matrices (Glass, 20kPa and 100kPa – **Figure 6A, 6D, 6E**), irregular two-dimensional meshes (lamellipodia) were observed due to the extension of the cytoskeletal structure. Pretreatment with Y-27632 led to an increase in the size of cells plated on the stiff glass (**Figure 6A**). Cells stimulated with CpG DNA or LPS were also imaged. Cells plated on stiffer matrices had extensive distribution of tubulin compared to those plated on more compliant matrices, reflecting the increase in cell footprint. This is in support of the expanding of the macrophages on stiff substrates as seen by the increase in the area covered by the actin filaments. Microtubule organizing centers were visible as spindles of tubulin filaments. Vinculin distribution in cells plated on gels and glass was punctate, corresponding to interactions between vinculin and the actin cytoskeleton which lead to formation of focal adhesion loci indicative of mechanosensing.

Figure 6: Inhibition of Rho kinases induces formation of filopodia and lamellipodia in RAW macrophages plated on gels and glass. Comparison of RAW 264.7 cells plated on (**A**) Glass, (**B)** 1kPa, (**C**) 5kPa, (**D**) 20kPa or (**E**) 100kPa gels with or without ROCK inhibitor Y-27632. Cells are stained for nuclei (DAPI, blue), actin (Alexa Fluor 488 phalloidin, green) and **tubulin** (Alexa Fluor 647, red) or vinculin (Alexa Fluor 647, red). Scale bars = 10 μm.

A

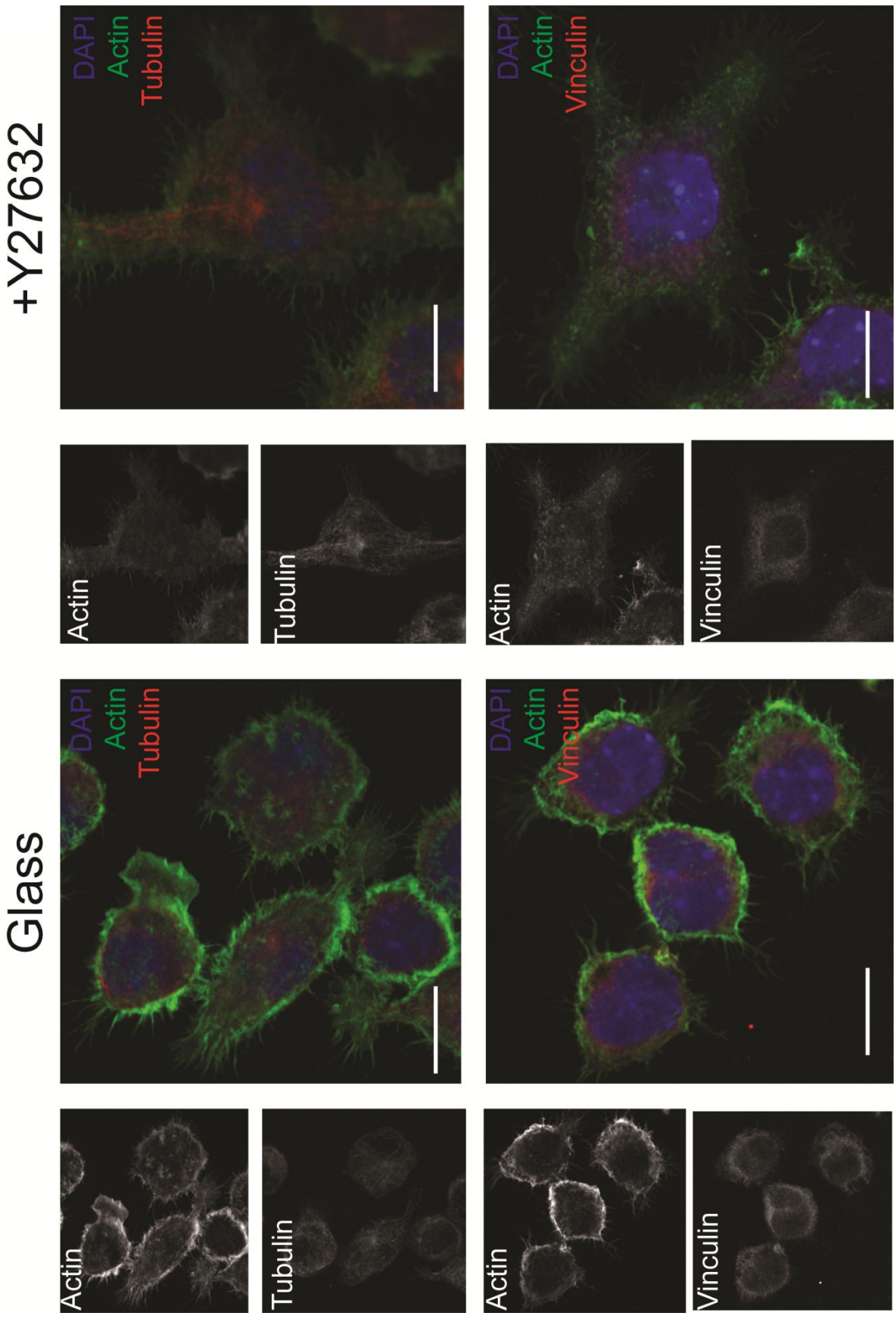
Glass
+Y27632
DAPI
Actin
Tubulin
Vinculin
Actin
Tubulin
Vinculin

Figure 6 (Continued)

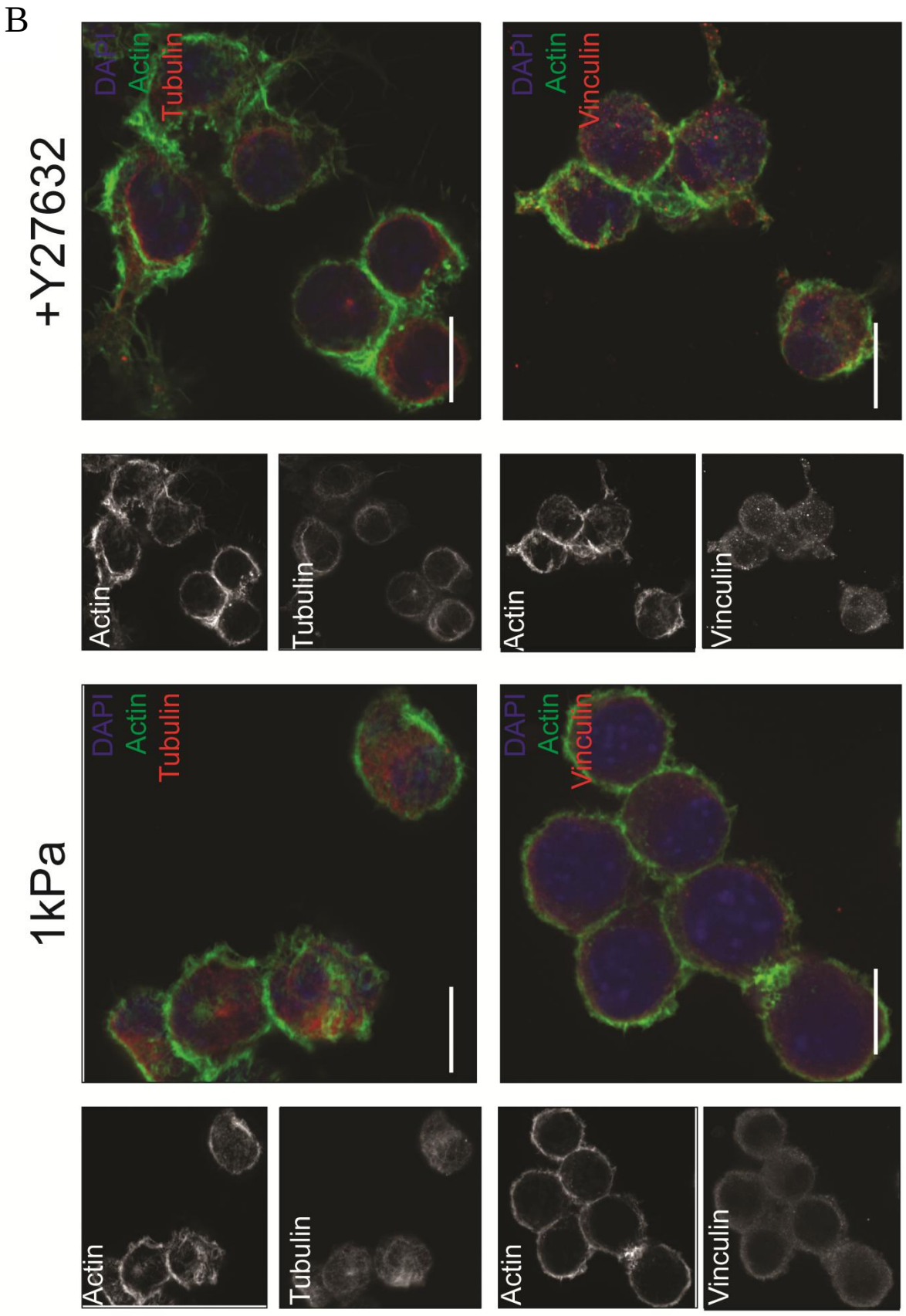

Figure 6 (Continued)

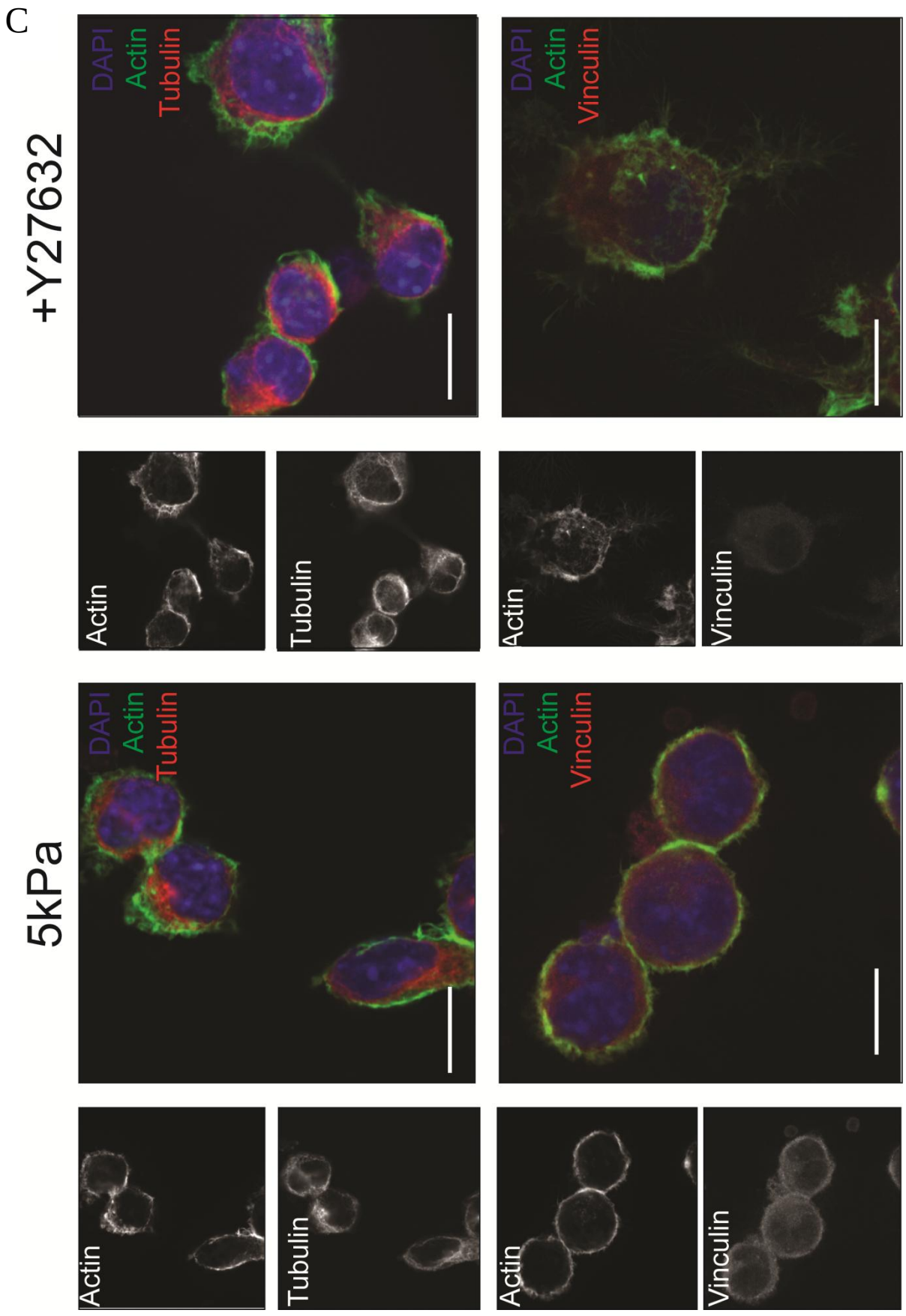

Figure 6 (Continued)

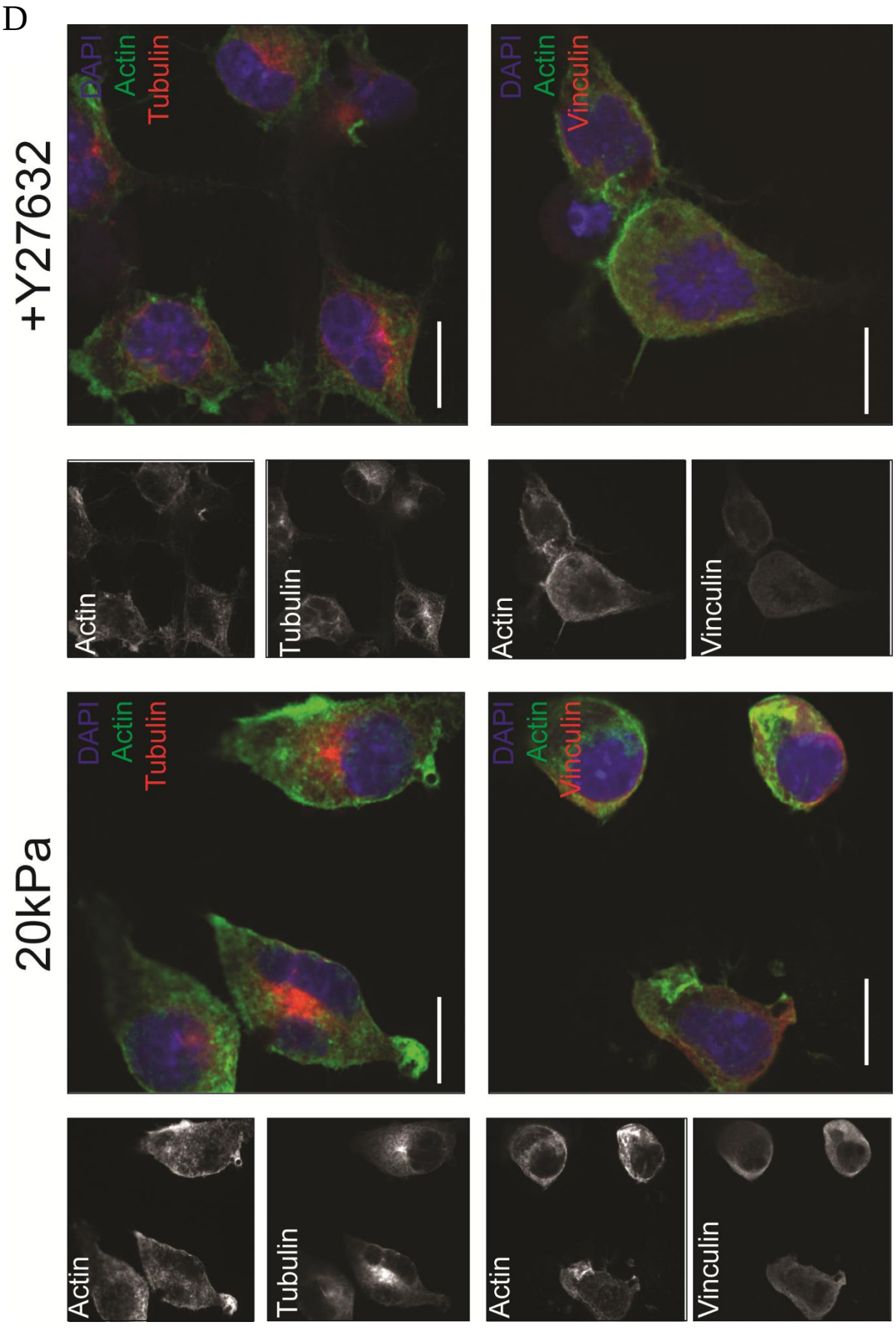

Figure 6 (Continued)

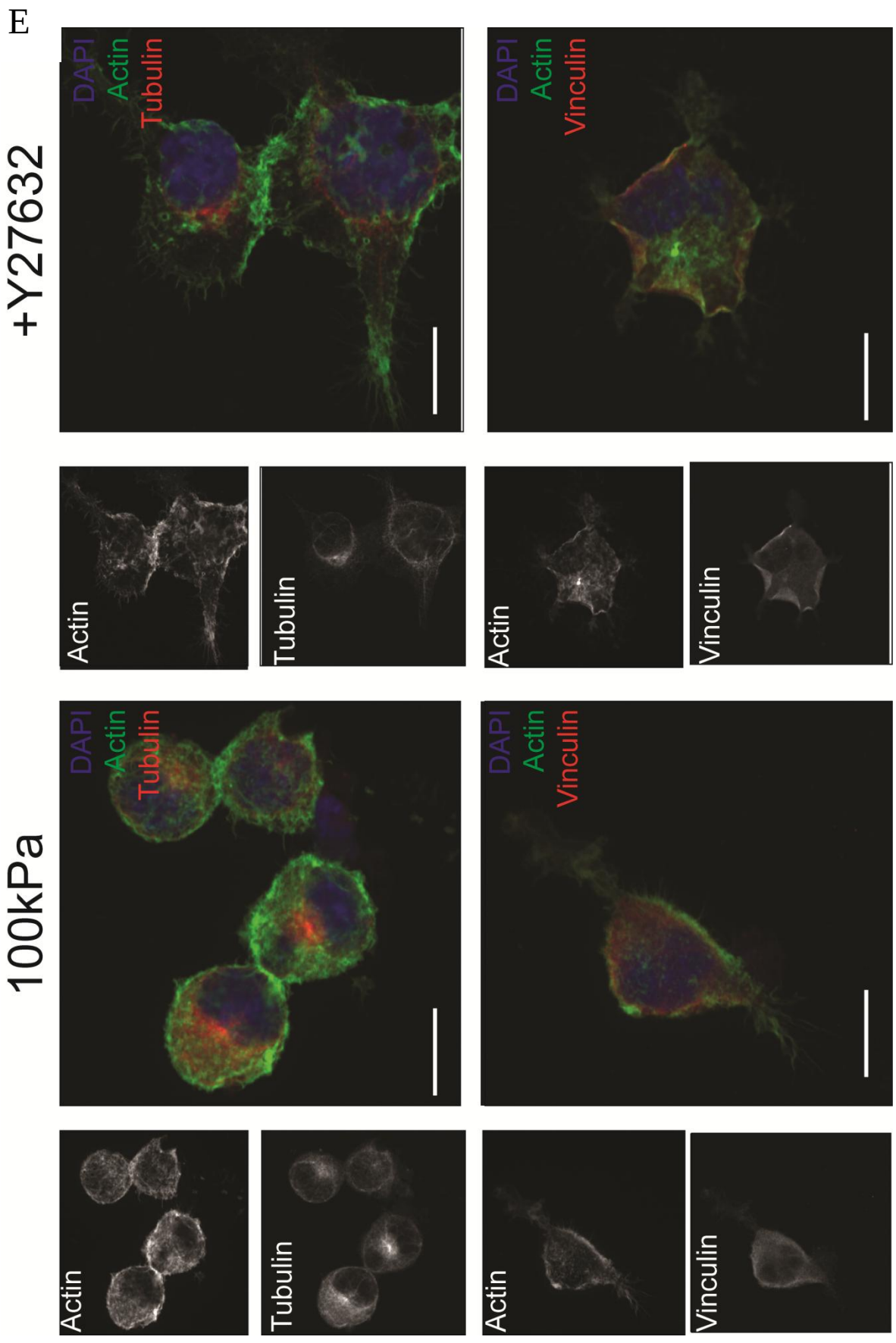

Macrophages pretreated with Y-27632 displayed a diffuse vinculin distribution, suggesting a loss of focal adhesion loci. Cells plated on 1kPa gel (**Figure 6B**) were the exception, showing more focal adhesion loci post-ROCK inhibition than without.

I next determined if inhibiting ROCKs affected macrophage TNF-α production in response to CpG DNA or LPS (**Figure 7**). TNF-α production was significant in cells plated on glass (**Figure 7A**), 20kPa gels (**Figure 7C**) and 1kPa gels (**Figure 7E**). Pretreatment with Y-27632 made a statistically significant difference in TNF-α production in response to CpG DNA or LPS stimulation in cases where the TNF-α secretion was significant. Y-27632 pretreatment lowered TNF-α response to CpG DNA stimulus in macrophages plated on 1kPa, 20kPa gels and glass. LPS response was significant only in the case of cells plated on glass, where Y-27632 pretreatment increased TNF-α production on stimulation.

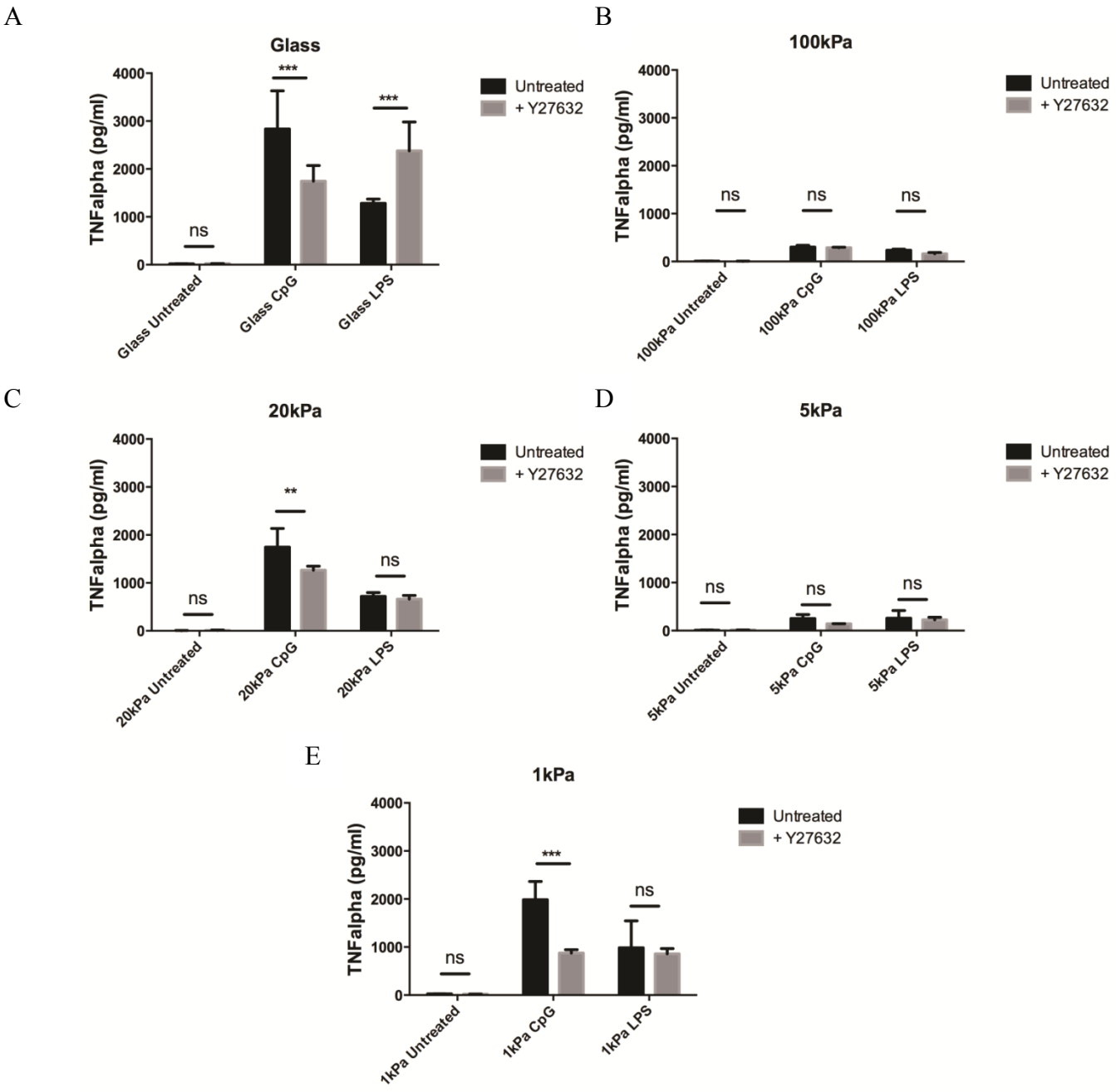

Figure 7: Proinflammatory cytokine production in macrophages is affected by pretreatment with rho kinase inhibitors. RAW 264.7 cells were plated on (**A-E**) Glass or 1, 5, 20 and 100kPa gels overnight and stimulated with CpG DNA or LPS, with or without pre-treatment with 10uM of ROCK inhibitor Y-27632 (30 min prior to stimulation) for 6 hours. Supernatants were collected after 6 hours of stimulation. Data was collected across two individual experiments consisting of 1) Glass, 1kPa and 5kPa gels and 2) Glass, 20kPa and 100kPa gels. Statistical significance was determined using the Holm-Sidak method in two-way ANOVA in GraphPad Prism, with alpha = %. ns = $P > 0.5$, ** = $P \leq 0.01$, *** = $P \leq 0.001$

3.5 Inhibition of actin filament re-polymerization does not significantly affect TNF-α production by activated macrophages.

Mechanosensing requires reconfiguration of the actin cytoskeleton for formation of adhesion and mechanotransduction contact points (Leung, 1996). To evaluate how cytoskeletal rearrangement affects the inflammatory response in macrophages, I tested the effect of actin polymerization inhibition on macrophage proinflammatory cytokine (TNF-α) production. In similar fashion to the ROCK inhibition experiment, RAW 264.7 cells were pre-treated with the actin polymerization inducer Jasplakinolide prior to stimulation with CpG DNA or LPS for nine hours. Jasplakinolide is a macrocyclic peptide natural product from the marine sponge *Jaspis johnstoni* that induces the polymerization of actin into filaments (F-actin) (Scott, 1988). It competitively binds to F-actin and irreversibly stabilizes it to form filaments (Bubb, 1994). Treatment of macrophages with Jasplakinolide would therefore provide a means to study the effect of loss of cytoskeletal reorganization capability on macrophage activation by comparing levels of inflammatory cytokine production. Analysis of supernatant from stimulated cells (**Figure 8A-E**) was inconclusive, as no significant data could be obtained. While cells plated on glass (**Figure 8A**) and 20kPa gels (**Figure 8C**) had a strong response in comparison to 100kPa (**Figure 8B**), 5kPa (**Figure 8D**) and 1kPa gels (**Figure 8E**), basal TNF secretion levels were also elevated, in comparison to basal response by cells in **Figure 7**. Jasplakinolide pre-treatment did have a statistically significant effect on TNF-α production in response to CpG DNA stimulation when compared to pre-treatment with DMSO (vehicle) in the case of 20kPa gels (**Figure 8C**). In the case of LPS, Jasplakinolide pre-treatment significantly reduced TNF-α production in cells plated on glass or 20kPa gels (**Figure 8C, 8E**).

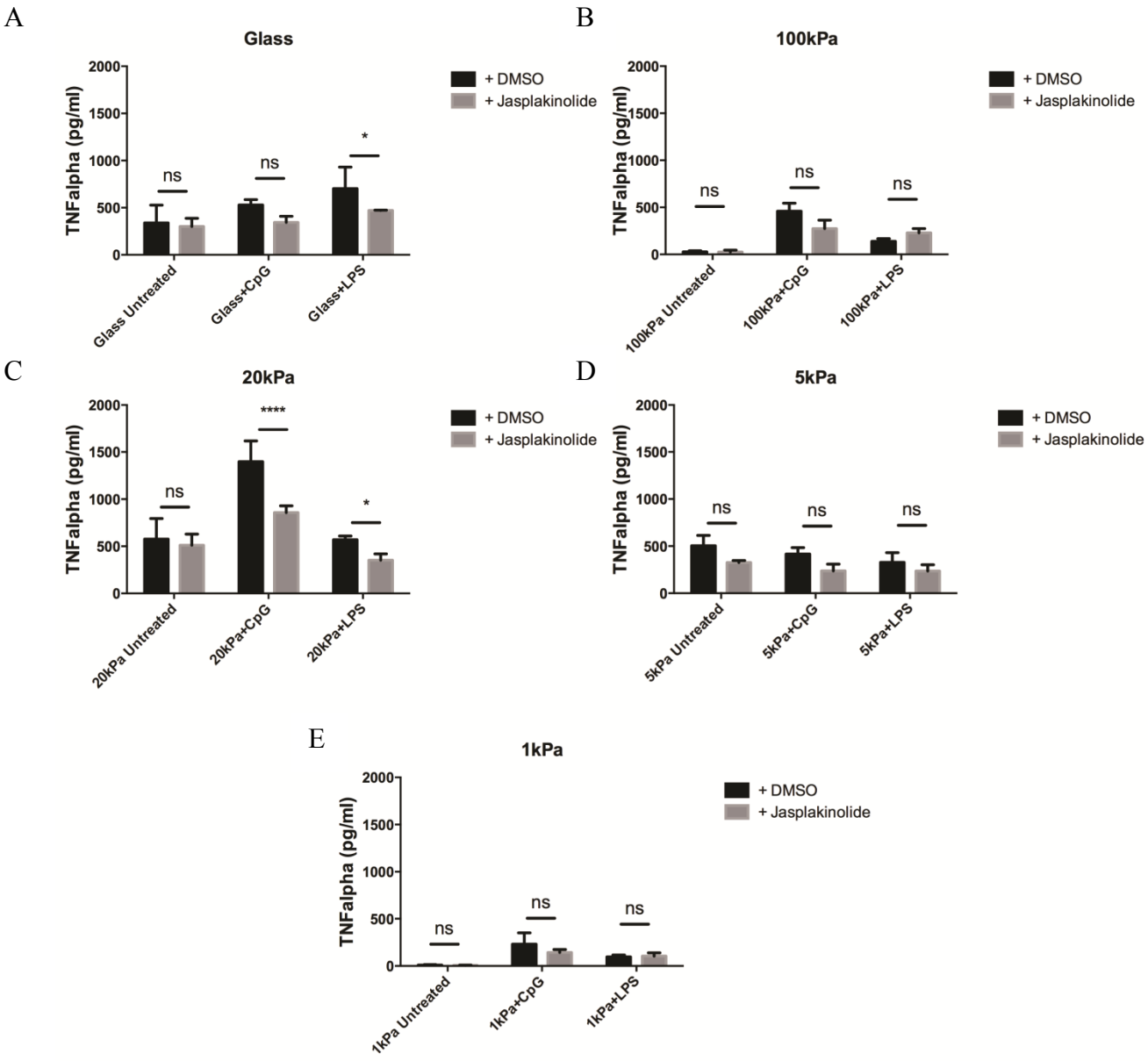

Figure 8: Effect of actin repolymerization inhibitor Jasplakinolide pretreatment on proinflammatory cytokine production in macrophages. RAW 264.7 cells were plated on 1, 5, 20 or 100kPa gels or glass overnight and stimulated with CpG DNA or LPS (with unstimulated controls) following pretreatment with DMSO vehicle or 0.5 uM Jasplakinolide dissolved in DMSO or un-pretreated control (pre-treatment done 30 min prior to stimulation). Supernatants were collected after 9 hours of stimulation and TNF-α was quantitated via ELISA (commercial kit). Data representative of two independent experiments. Statistical significance was determined using the Holm-Sidak method in two-way ANOVA in GraphPad Prism, with alpha = 5%. ns: $p > 0.5$, *: $p < 0.05$, ****: $p < 0.0001$.

3.6 Increase in substrate stiffness increases Rho kinase expression in macrophages.

ROCKs induce the formation of actin stress fibers and focal adhesions by phosphorylating the myosin light chains (MLC) (Leung, 1996), an act in which the ROCKs become phosphorylated. To determine whether mechanosensing-driven rearrangement of the actin cytoskeleton requires ROCK, I assessed the level of ROCK expression and phosphorylation in RAW 264.7 macrophages plated on 1, 5, 20 or 100kPa gels or glass coverslips via Western Blot. Immunoblotting of lysine with antibodies against ROCK1 and phospho-ROCK1 revealed an increase in ROCK1 protein in cells plated on stiffer substrates (**Figure 9A**). pROCK1 detection was insufficient to draw conclusions about degree of ROCK1 phosphorylation in the cells. Densitometry analysis of the ROCK1 immunoblot bands normalized to α-tubulin expression levels (**Figure 9B**) showed that ROCK1 expression in cells appeared to increase with increase in substrate stiffness (with the exception of cells plated on 100kPa gel). Densitometric analysis of the degree of ROCK1 phosphorylation (pROCK1 intensity/ ROCK1 intensity) (**Figure 9C**) was inconclusive due to the low detection of pROCK1 in the immunoblot. Therefore, ROCK1 expression in macrophages may increase with increase in substrate stiffness, but whether ROCK1 phosphorylation (and hence activation) increases as well is as yet unclear.

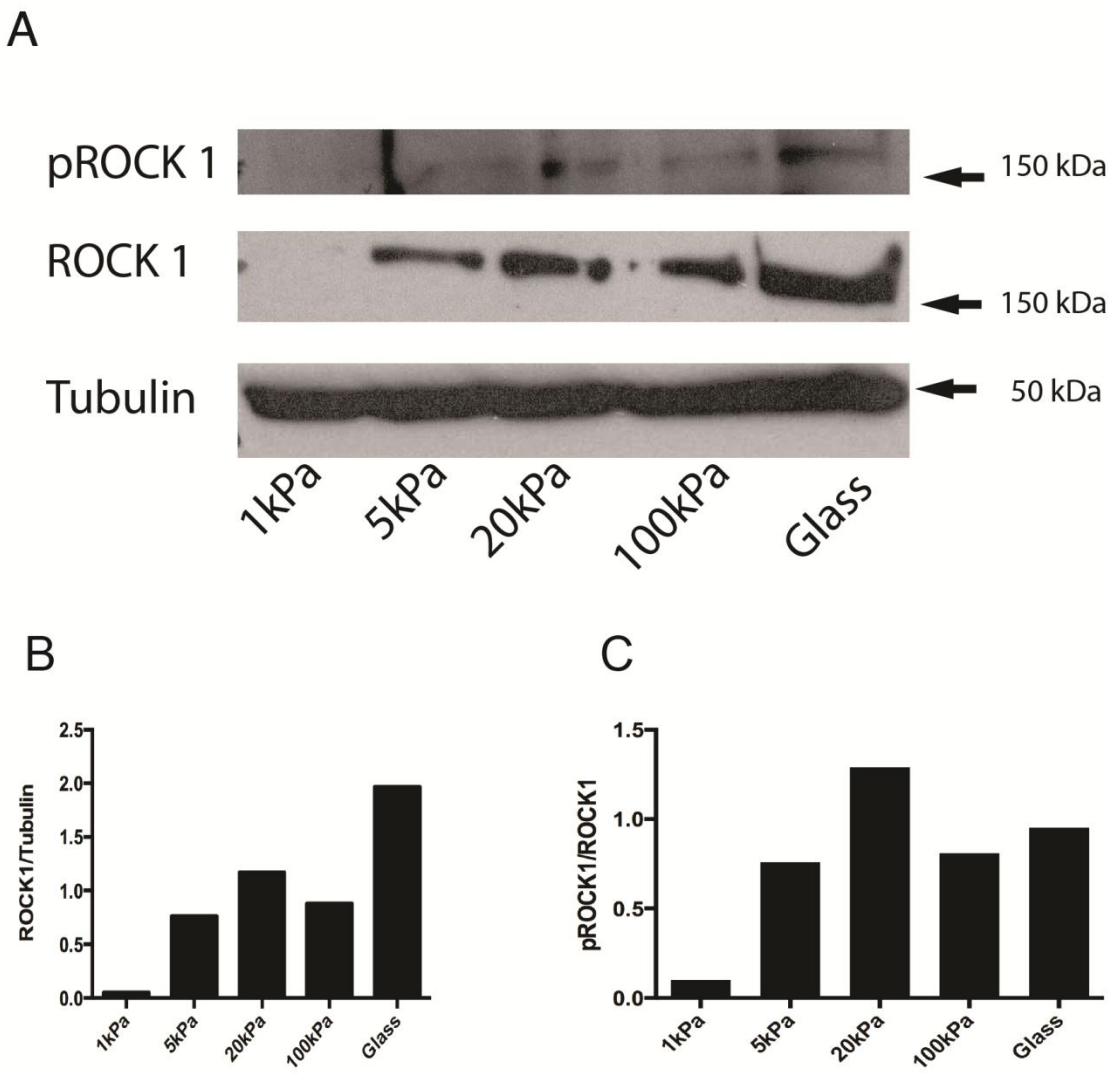

Figure 9: ROCK phosphorylation in RAW 264.7 macrophages increases with increase in substrate stiffness. (A) RAW 264.7 cells were incubated overnight on 1, 5, 20, or 100 kPa PAA gels or glass. Cells were lysed in lysis buffer and lysate probed for ROCK1 and phospho-ROCK1 (Cell Signaling C8F7 Rabbit anti-ROCK1 antibody and BioSS bs-4063R Rabbit anti-phospho-ROCK1 antibody respectively, Southern Biotech Goat anti-Rabbit HRP secondary antibody) as well as for tubulin (eBiosciences 14-4502 anti-alpha tubulin). **(B)** Immunoreactive band intensity of ROCK1 was quantified and normalized to that of tubulin loading control in ImageJ. (**C**) Degree of ROCK1 phosphorylation (pROCK1/ROCK1 band intensity) was quantified in ImageJ and plotted in GraphPad Prism.

CHAPTER 4

DISCUSSION

4.1 Summary of findings

Macrophages are one of the primary driving factors in the progression of atherosclerotic plaques. Lipid buildup in the subendothelial regions of arteries 'activates' the overlying endothelium, leading to recruitment of blood-borne monocytes to the accumulation site. Normally, monocytes then differentiate into macrophages that secrete the anti-inflammatory cytokine IL-10 and clear the lipids and apoptotic cells accumulated in the region. If the individual has multiple factors predisposing them for atherosclerosis; however, the lipid buildup becomes in excess of the macrophages' capacity to clear them. At this point the macrophages begin to take up lipid in excess of their capacity to clear it and turn into macrophage foam cells, which accumulate in the buildup site and eventually undergo apoptosis. Failure of other macrophages to efficiently clear these apoptotic cells (efferocytosis) leads to secondary necrotic death, which is highly inflammatory and promotes development of a necrotic core. While normal efferocytosis would promote resolution of inflammation via production of IL-10 and TGF-β by macrophages, impaired efferocytosis exacerbates inflammation due to macrophages that respond to toxic lipids and apoptotic cell debris by producing TNF-α and other proinflammatory cytokines. As plaque development progresses, the necrotic core increases in size while the overlying fibrous cap thins out due to degradation by matrix metalloproteases (MMPs). These thin caps are unstable and can rupture leading to thrombotic events (Nagase, 2006; Newby, 2007; Chowdhary, 2006).

We can thus see that macrophages play multiple vital roles in atherogenesis, and there are therefore multiple pathways that could be targeted to interrupt the inflammatory cycle (e.g., monocyte recruitment, macrophage polarization, efferocytotic activity etc.). Development of effective therapies necessitates proper investigation and definition of the role(s) played by macrophages at each step of atherogenesis. Existing approaches such as transcriptome analysis have provided multiple differentially regulated genes in atherosclerosis, but the cellular- and tissue-level complexity of an atherosclerotic lesion lead to difficulties in proper mapping of gene expression profiles to the appropriate cells within the tissues. While technologies such as laser capture microdissection allow isolation of individual parts of the lesion such as the necrotic core and the fibrous cap and help partially overcome the mapping problem, there is still a need to be able to control and mimic the tissues' mechanical properties, which can vary from very compliant (necrotic core) to very stiff (fibrous cap). Since growth environment stiffness has been known to play a role in fate determination of mesenchymal stem cells during differentiation (Engler, 2006), there is a strong need to determine the relative role of macrophage mechanosensing in the regulation of atherosclerosis. In this thesis, I examine the effect of substrate stiffness on macrophage function: inflammatory cytokine (TNF-α) production, microbial phagocytosis and lipid uptake and clearance. I also examine the effects of inhibition of rho kinases (which play an important role in mediation of mechanosensing pathways) and inhibition of actin polymerization on cytokine production profiles.

The first task was to examine the effect of compliant vs. stiff substrates on macrophage morphology and cytokine production. Previous research had been conducted detailing the effect of substrate stiffness on different cell types such as murine aortic smooth muscle cells (Engler

2004), alveolar macrophages (Fereol, 2006) and primary bone marrow-derived macrophages (Blakney, 2012). To develop a proper understanding of the effects of substrate stiffness on macrophages' role in atherosclerosis progression, it was necessary to develop a model to study monocyte-derived macrophages *in vitro* that would accurately mimic the range of tissue stiffnesses encountered in atherosclerotic lesions. The polyacrylamide gel model used in my studies is highly tunable and versatile (as the stiffness of the gel can be adjusted to defined values by changing the acrylamide/bisacrylamide ratio to predefined values – Pelham, 1997) , allowing me to cover the spectrum of stiffness encountered in atherosclerosis with minimal adjustment. However, the polyacrylamide gel model has many limitations: it is not a biological material and thus must be functionalized and coated with a biological matrix to promote cell adhesion, limiting its usefulness to 2-dimensional studies which only roughly approximate *in vivo* conditions. The polyacrylamide matrix is also very hygroscopic in nature, and is thus prone to swelling in aqueous conditions which can change the actual stiffness of the gel and exert additional undesirable mechanical stress on cells. Alternatives to the polyacrylamide gel system include use of collagen-based, gels which are biological in nature and provide better approximate biological conditions. The most ideal choice would be matrigel, which is a gelatinous protein mixture of laminin, entactin and collagen secreted by Engelbreth-Holm-Swarm mouse sarcoma cells (Hughes, 2010). This mixture closely resembles the extracellular matrix of many living tissues and acts as a viable culture medium when perfused with the appropriate nutrients. Additionally, its mechanical properties are highly tunable and it is capable of self-assembly at body temperature (37^0C) into solid form but is a liquid at lower storage temperatures (4^0C). However, since the matrigel is composed entirely of ECM proteins, substrate stiffness cannot be uncoupled from ECM protein concentration. Cells form mechanosensing interactions via

integrin-mediated adhesion to ECM protein; therefore measuring the effect of substrate stiffness on macrophage behavior independent of adhesion strength will be difficult.

Here, I have shown that cells plated on softer gels (20kPa) secrete higher basal amounts of the proinflammatory cytokine TNF-α , as well as upon stimulation with CpG DNA (simulating the pro-inflammatory effect of cellular debris present in advanced atherosclerotic plaques) than cells plated on stiff glass, although the final fold increase from basal levels is lower. This finding supports a model where macrophages that are exposed to the compliant lipid-rich environment of atherosclerotic lesions are more likely to produce pro-inflammatory cytokines when they come into contact with apoptotic cells and inflammatory products of apoptosis in the lesion, fueling further inflammation.

Comparison of phagocytotic activity across cells plated on gels of varying stiffnesses revealed that cells plated on softer substrates exhibited lower rates of bioparticle phagocytosis, possibly due to the increased surface area of cells plated on stiffer substrates increasing the chance of encountering a bioparticle. While microbial phagocytosis in macrophages is different from apoptotic cell phagocytosis (highly proinflammatory compared to anti-inflammatory), this is still strong evidence implicating that macrophage response to physical substrate stiffness plays a role in regulation of macrophage phagocytosis.

Lipid uptake and clearance were also affected by substrate stiffness. Oleate uptake was increased in cells plated on softer gels and occurred earlier than in cells plated on stiffer gels and glass. Lipid clearance during the 24-hour observation period was adversely affected on softer gels, with

significantly higher volume of lipid being retained after 24 hours. This suggests that lipid loading is accelerated in early atherosclerotic fatty streaks and promotes foam cell formation, while in advanced atherosclerotic lesions the stiffness of the fibrotic cap discourages lipid uptake in macrophages and causes lipid accumulation in the lesion core.

The observed effects of substrate stiffness on macrophage morphology and cytokine production led me to investigate the effects of disruption of mechanosensing on macrophages. Rho kinases (ROCK 1 & 2) play a vital role in mediation of mechanosensing pathways and were chosen as the targets. Pretreatment of RAW264.7 cells with the pharmacological ROCK inhibitor Y-27632 followed by stimulation with CpG DNA or LPS reduced the sensitivity of the RAW cells to CpG DNA stimulation when the cells were plated on glass or 20kPa/1kPa gels (response from cells on other gels was inconclusive). Response to LPS stimulus was significantly different (elevated) in the case of cells plated on glass only. Inhibition of ROCK appeared to increase the cell size on higher stiffnesses. This suggests that ROCK-associated mechanosensing of substrate stiffness plays a role in determining the magnitude of pro-inflammatory response in macrophages, in a manner specific to the type of inflammatory stimulus presented to the macrophages. Inhibition of ROCK activity may therefore retard the substrate stiffness-associated changes in macrophage inflammatory profiles.

An experiment was designed to test the effect of an actin repolymerization inhibitor Jasplakinolide on mechanosensing. However, pretreatment of RAW 264.7 cells with Jasplakinolide followed by stimulation with CpG DNA or LPS did not provide sufficient data to determine whether TNF-α production is affected by inhibition of actin repolymerization, other

than a decrease in TNF production in cells on 20kPa gels when stimulated with either CpG or LPS, or in cells on glass stimulated with LPS. While my results were inconclusive, further investigation may reveal the effect of inhibiting actin cytoskeletal rearrangement in response to changes in substrate stiffness on macrophage inflammatory response.

I also analyzed the level of expression and degree of phosphorylation (signifying activation) of ROCK1 in macrophages plated on the various substrates (1, 5, 20 and 100 kPa gels and glass) by resolving the whole cell lysate of the plated cells via SDS-PAGE and immunoblotting for ROCK1 in its phosphorylated and unphosphorylated forms. It was found that ROCK1 expression increased with increase in substrate stiffness, but immunoblot of phospho-ROCK1 was inconclusive; therefore effect of stiffness on ROCK1 activity cannot yet be defined.

4.2 Macrophages sense the stiffness of their growth substrate and modulate proinflammatory cytokine production accordingly.

Primary bone marrow-derived macrophages plated on compliant (20kPa) gels adopted a smaller footprint with short, singular projections while macrophages on glass occupied a larger footprint and had longer, 2-dimensional projections (**Figure 2**). Macrophages on compliant gels also had higher background levels of TNF-α, and when stimulated with CpG DNA, produced significantly more TNF-α than macrophages on highly rigid glass (**Figure 3**), a finding that is consistent with a previous study in murine bone marrow-derived macrophages plated on polyethylene glycol (PEG-RGD) hydrogels (Blakney, 2012) where relative TNF-α gene expression levels were higher in cells plated on more compliant gels. Fold increase in TNF production upon CpG stimulation was lower in cells plated on gel, due to the relatively high

basal response. The response was specific for gel stiffness and not biomatrix chemistry, since the response of cells on 20 kPa gels crosslinked with BSA or poly-L lysine was statistically significantly greater than on the corresponding BSA/PLL-coated glass coverslips ($p<.001$). These results support previously published studies on other macrophage types and provide evidence for substrate stiffness playing an important role in modulation of proinflammatory cytokine production via mechanosensing. The findings support the idea that macrophages existing in lipid- and cellular debris-rich atherosclerotic lesions contribute to inflammation, as they are likely to produce more proinflammatory cytokine in a compliant environment.

4.3 Macrophage bacterial phagocytosis increases with substrate stiffness.

The observed reduction in macrophage footprint and increase in proinflammatory cytokine production on more compliant substrates correlated with reduced microbial phagocytosis. Importantly, the alterations in phagocytotic activity were not unique to the 20kPa gels and were also observed on even more compliant 5kPa gels – effectively, microbial phagocytosis was maximized on glass compared to the limited uptake when on gels, independent of bioparticle dosage (**Figure 4**). This increase may also be due to the increased surface area presented by the macrophages plated on glass, which would increase the chance of encountering and engulfing the bioparticle. This increase in phagocytotic activity may help explain to the observed lower efferocytotic efficiency of macrophages in the compliant necrotic core of advanced lesions, leading to buildup of apoptotic cells and toxic cellular debris, which leads to further inflammation. It is worth noting that phagocytosis of bacteria and yeast is highly proinflammatory and relies on different receptors than phagocytosis of apoptotic cells, which is anti-inflammatory (Huynh, 2002). Therefore, loss of efferocytotic activity in the lesion core

promotes inflammation through both buildup of proinflammatory cellular components and loss of anti-inflammatory cytokine. These data strongly implicate macrophages response to physical stiffness as a mechanism for regulating phagocytosis and point to a potential therapeutic avenue for controlling atheroprogression via modulation of phagocytosis. Further research would include the direct study of efferocytotic activity in primary bone marrow-derived macrophages plated on gels and incubated with apoptotic cells, analyzing efferocytotic efficiency and cytokine production variability across substrate stiffness, dosage levels and incubation periods.

4.4 Macrophage lipid uptake is dependent on substrate stiffness.

Primary bone marrow-derived macrophages plated on 20kPa gels or glass developed lipid droplets at six hours and very few lipid droplets were still detectable by 24 hours. In contrast, macrophages plated on 5kPa gels were loaded with lipid droplets by 2 hours (**Figure 5A**) and still contained significant numbers of lipid droplets at 24 hours (**Figure 5B**). After 2 hours, small lipid droplets (<2 μm dia.) were visible in the cells, but by 24 hours, large lipid droplets (>5 μm dia.) were visible (**Figure 5B**). Statistical analysis of lipid droplet counts across the three substrates over time showed that lipid uptake and retention was indeed higher in cells plated on the softest (5kPa) substrate (**Figure 5C, D**). These data suggest that lipid uptake and efflux are regulated by mechanosensing, such that macrophages grown on compliant matrices take up more quickly, and retain larger volume of lipids, than those grown on stiffer substrates. It should be kept in mind that uptake of normal lipids is a beneficial function of macrophages while uptake and storage of oxidized lipids results in foam cells and progression of atherosclerosis. This supports a model where macrophages alighting on healthy, compliant arterial tissue have efficient lipid uptake but get overloaded with lipid in the lipid-rich fatty streak tissue of early

atherosclerotic lesions, forming large foam cells. In later stages of the lesion, the stiffness of the fibrotic cap lowers lipid uptake in neighboring macrophages, leading to increased lipid buildup in the lesion core. In addition, decrease in free cholesterol efflux or ACAT function in lesional macrophages (Yvan-Charvet, 2007; Zhu, 2008; Tang, 2009) may lead to macrophage death due to cholesterol-induced toxicity and subsequent increase in apoptotic cell numbers, forming the necrotic core seen in late-stage plaques.

4.5 Inhibition of rho kinases affects cell morphology and TNF-α production.

Rho kinases (ROCK) are downstream effectors of the small GTPase Rho and phosphorylate LIM kinase (which in turn phosphorylates cofilin and inactivates its ability to inhibit actin depolymerization) (Maekawa, 1999) as well as myosin light chain kinase (increasing myosin II ATPase activity and shorten actin fibers) (Wang, 2009). ROCKs have been established in literature as playing a role in macrophage migration in three-dimensional environments (Van Goethem, 2010), efferocytosis (Tosello-Trampont, 2003) and foam cell formation (Wang, 2008). This supports the idea that ROCKs are involved in the regulation of pro-atherogenic macrophage functions via regulation of macrophage mechanosensing. Efferocytosis is enhanced when RhoA-mediated signaling is inhibited and inhibited upon overexpression of constitutively active RhoA (Tosello-Trampont, 2003). In bone marrow-derived macrophages, ROCK1 is necessary for movement into atherosclerotic lesions and for foam cell formation (Wang, 2008). ROCK regulates several cytoskeletal processes including cytoskeletal tethering, which is the major mechanism for mechanotransduction in response to substrate stiffness, and is thus a good candidate for studies examining the role of mechanosensing in proatherogenic functions of macrophages. The chemical compound Y-27632 ((1R, 4r)-4-((R)-1-aminoethyl)-N-(pyridin-4-yl)

cyclohexanecarboxamide) inhibits p160ROCK (Uehata, 1997) and is thus an ideal biochemical tool to study ROCK. In this study, it was found that pretreatment of RAW264.7 cells with Y-27632 resulted in an increase in cell size in macrophages plated on the stiffer substrates (**Figure 6**). This may be explained by the loss of mechanosensing in the cells leading to formation of new cytoskeletal projections to reacquire mechanical cues from the environment. Resolution of vinculin protein (involved in the formation of focal adhesion plaques that link integrin adhesion molecules to the actin cytoskeleton) in the cells reveals a loss of the discrete punctate distribution of vinculin in the Y-27632-treated cells plated on glass (**Figure 6A**), suggesting that cellular adhesion and thus mechanosensing has been successfully disrupted. This disruption is not consistent, as vinculin distribution was not diffused in the case of other substrates (in the case of 1kPa gel (**Figure 6B**), the vinculin distribution is enhanced, suggesting that mechanosensing is not disrupted). The tubulin network in cells is unaffected by exposure to Y-27632 except for the formation of microtubule-organizing centers (MTOCs) prominently visible in the cells plated on softer gels (1kPa and 5kPa) (**Figure 6A**). This may be explained by the fact that Y-27632-induced loss of focal adhesion bodies affects cellular adhesion most adversely in cells on compliant gels, due to the overall smaller number of existing adhesion points compared to stiffer gels making the loss a greater percentage of the total. The formation of the MTOC is the event that initiates *de novo* formation of additional microtubules to restore structural rigidity and consequently recover cellular adhesion. These changes were not observed in all cells plated on the same substrate and were not found in all substrates, suggesting that ROCK inhibition may not have been universal. There is therefore a need to find the optimal conditions for comprehensive ROCK inhibition by Y-27632.

ELISA analysis of TNF-α production in the RAW cells after Y-27632 pretreatment and stimulation with CpG DNA or LPS (**Figure 7**) did not show any significant change in TNF-α compared to cells untreated with Y-27632 other than in the conditions where TNF-α production was already high (in which case ROCK inhibition reduced the TNF-α response to CpG DNA stimulation and increased the LPS response). This could potentially be due to the inflammatory stimulus being too low to provoke a significant response. Alternatively, the RAW264.7 cells (which were chosen for this and other experiments rather than primary macrophages due to time and logistical constraints) being a differentiated, immortalized cell line and therefore not as sensitive to environmental stiffness variation and inflammatory stimulus could contribute to the seeming insensitivity to Y-27632 pretreatment. Both theories can be tested in the future by using bone marrow-derived macrophage populations instead and administering the ROCK inhibitor earlier in the process of adherence/acclimatization to the substrate, as well as ensuring that the population of available cells as well as the dose of inflammatory stimulant is sufficiently large to generate a distinct response. The difference in CpG and LPS response may be due to the fact that ROCK is a downstream effector of RhoA, which is a target for rapid activation by LPS (Chen, 2002) in order to regulate NF-κB activation. Stimulus-dependent complex formation between active RhoA and the novel protein kinase Cζ (PKCζ) was observed to be essential for regulating NF-κB activation (Chen, 2005). LPS-induced activation of RhoA, in the absence of the downstream target ROCK, may cause increased NF-κB activation and TNF-α production, explaining the increase in TNF production in macrophages treated with the ROCK inhibitor. While the effect of CpG DNA stimulation of TLR9 in lesional macrophages has not been fully defined, $TLR9^{-/-}$ mice recover better from a transverse aortic constriction model of heart failure

(Oka, 2012). It is possible that TLR9 plays an atheroprotective role similar to TLR7, whose deficiency enhances lesion development in *ApoE*-deficient mice (Salagianni, 2012).

TNF-α production in cells plated on 20kPa gels was significantly higher than that in cells plated on all other gels, distinct from the trend of increased TNF-α production on more compliant gels. This anomaly may be correlated to the increased swelling observed in 20kPa gels compared to 1, 5 and 100kPa gels – the additional shear stress and strain exerted on the cells due to the swelling could be a potential cause of cytokine release in response to stress, as it has been previously reported that mechanical stress induces TNF-α production in the monocyte-like cell line THP-1 (Kim H.G, 2008). The cause of the swelling is unknown, but may be due to the specific ratio of acrylamide and bisacrylamide required to make a 20kPa gel causing an increase in water absorption capacity.

4.6 TNF-α secretion is not significantly affected by Actin repolymerization inhibition.

Mechanosensing in cells requires modification of the actin cytoskeleton in order to generate the actin projections that form the focal adhesion points for rigidity sensing. In this experiment, RAW264.7 cells plated on 1, 5, 20 or 100kPa gels or glass were pretreated with Jasplakinolide prior to stimulation with CpG DNA or LPS. TNF-ELISA of cell supernatant revealed mostly insignificant difference between cells pretreated with Jasplakinolide and cells treated with DMSO vehicle alone, except in the cases of cells plated on 20kPa gel and stimulated with either CpG DNA or LPS, and cells plated on glass and stimulated with LPS (**Figure 8**). In all cases, the basal, unstimulated response was also high, suggesting that the cells did not receive sufficient inflammatory stimulus or the RAW264.7 cells being a stable, immortalized cell line contributed

to the seeming insensitivity to Jasplakinolide pretreatment. This could be also be tested by using bone marrow-derived macrophages instead and beginning the pre-treatment earlier in the process of adherence, for a longer duration with a sufficiently large cell population. Jasplakinolide efficacy could also be tested by evaluating apoptotic rates in the various cell populations (since Jasplakinolide has been shown to enhance the interleukin-2 apoptotic signal in CTLL-20 interleukin-2-dependent T cells (Visegrady, 2005)), and determining whether substrate stiffness affects Jasplakinolide-induced apoptosis rates.

4.7 Rho kinase expression is increased in cells plated on stiffer substrates.

It was observed that expression of Rho kinase 1 (ROCK1) was highest in cells plated on glass, with the level of expression decreasing with the decrease in substrate stiffness (**Figure 9**). pROCK1 expression was too low to make any conclusions regarding the effect of substrate stiffness on ROCK1 phosphorylation and hence activity. This may be because the lysates were collected after the cells had been incubated overnight on the substrates: ROCK1 phosphorylation may have occurred within the first few hours of plating as the macrophages sensed their new environment. Neither ROCK1 nor pROCK1 were detectable in the lysate from cells plated on 1kPa gel. Since tubulin expression was consistent across all the samples, lack of ROCK1 detection is unlikely to be due to failure to detect protein. A likely explanation would be that initial mechanosensing of the soft 1kPa substrate was insufficient to drive formation of additional focal adhesion loci in the cytoskeleton. Therefore, the need of expression of additional Rho kinase over the (undetectable) constitutively present amount to form the adhesion bodies was absent. In contrast, the cells plated on 100kPa gel and glass generated large numbers of focal adhesion bodies and underwent extensive actin cytoskeletal rearrangement, thus necessitating

increased expression of ROCK1 We have previously seen that RAW 264.7 macrophages plated on stiffer substrates also show increased complexity in vinculin structures, i.e., increased number of focal adhesion points and thus mechanosensing capability (**Figure 6A, E**). Activation of Rho signaling is necessary for formation of focal adhesions (Ridley, 1992). Therefore, our findings provide further evidence for increased mechanosensing in macrophages plated on stiffer surfaces and a corresponding lower degree of mechanosensing on more compliant substrates. In conjunction with the data showing an increase in TNF-α production from cells plated on compliant gels, this is additional support for the theory that compliant environments promote pro-inflammatory cytokine expression profiles in macrophages. Rho kinases are known to regulate macrophage motility (Van Goethem, 2010) and ROCK1 deficiency is known to impair monocyte-macrophage chemotaxis as well as hinder foam cell formation via reduced lipid uptake (loss of ability to traffic lipid-containing vesicles along the cytoskeleton), thus reducing foam cell accumulation and atherosclerotic lesion progression (Wang, 2008). Inhibition of ROCK-mediated signaling also enhances uptake of apoptotic cells (Tosello-Trampont, 2003). Thus, ROCK1 and its downstream effectors could be potential therapeutic targets for the treatment of atherosclerosis.

4.8 Model for macrophage involvement in the progression of atherosclerotic plaque.

My research findings (summarized in **Figure 10**) demonstrate that surface rigidity regulates macrophage cytokine production. Bacterial phagocytosis and retention is enhanced in cells plated on stiffer substrates. Macrophages uptake and retain significantly more model lipid on compliant gels. While loss of mechanosensing via ROCK inhibition or actin repolymerization inhibition does not directly affect production of inflammatory cytokine TNF-α, the ability of cells to

recover and re-establish cellular adhesion decreases with increase in substrate compliance. These data add to our understanding of the following model (**Figure 11**) where macrophages react to the high compliance conditions of normal arteries or early lipid-rich atherosclerotic lesions by increasing efferocytotic activity and lipid uptake (**Figure 11, panel 1**). Once lipid accumulation exceeds the clearance capability of the macrophage population, the compliant environment enables increased lipid uptake but hinders lipid clearance, leading to formation of foam cells that add to the load of cells marked for apoptosis and exceed the efferocytotic capacity of the cells, which has been reduced due to the compliant environment (**Figure 11, panel 2**). This leads to buildup of lipids, cellular debris and toxic products of apoptosis, which stimulate proinflammatory cytokine production in macrophages and lead to the formation of a pliable necrotic core. In advanced lesions, the fibrotic cap is generated by surrounding endothelial cells, smooth muscle cells and macrophages in order to restore the mechanical integrity of the inflamed lesion. The cap provides a stiff environment for the functioning macrophages at the periphery of the necrotic core, reducing efferocytosis and anti-inflammatory cytokine production, leading to further inflammation and secondary necrosis, enlarging the necrotic core (**Figure 11, panel 3**). Increased production of matrix metalloproteases by macrophages (arising from monocytes which are continuously being recruited to the lesion site) promotes degradation of the fibrotic cap, increasing the likelihood of plaque rupture and subsequent thrombosis, which can be fatal (**Figure 11, panel 4**).

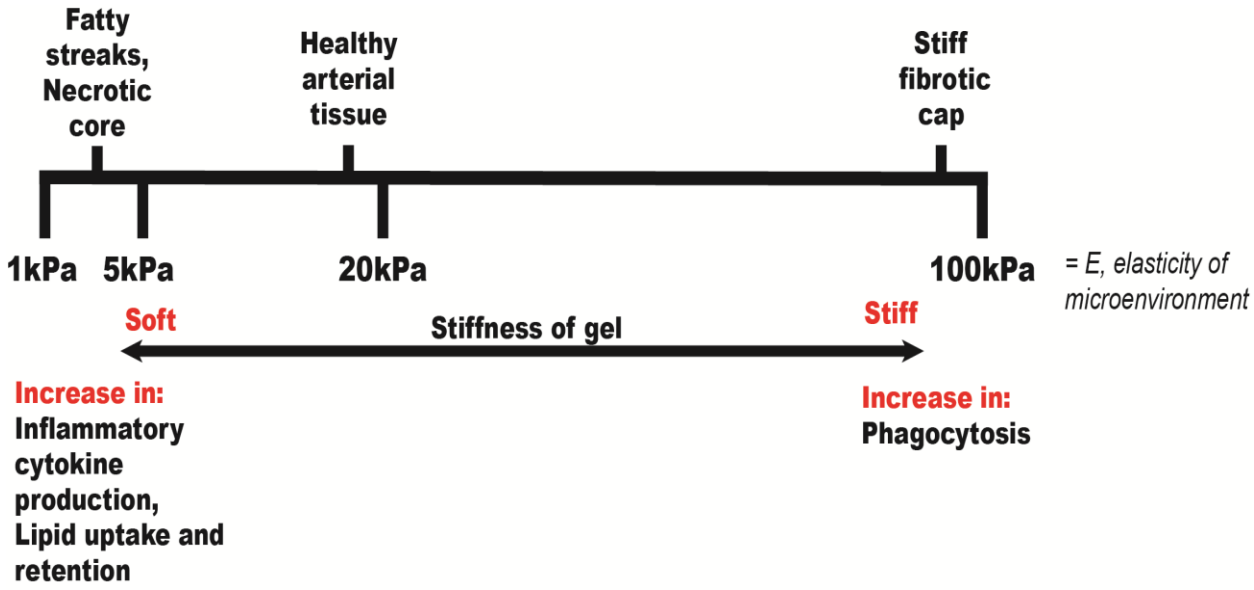

Figure 10: Summary of Research findings. Elasticity of tissues calculated from Tracqui, J. Struc. Biol., 2011.

Figure 11: Model of macrophage involvement in the progression of atherosclerotic plaque. On compliant normal arteries or early fatty streaks (**panel 1**), monocytes are recruited to the sites of excess lipid buildup, where they give rise to macrophages that take up excess lipid and efferocytose apoptotic cells. At this stage, macrophages produce anti-inflammatory cytokine (TGF-β) in larger amounts and limit lesion formation. Once lipid accumulation exceeds clearance capability of the resident macrophages (**panel 2**), lipid clearance falls behind lipid uptake, leading to formation of foam cells which in turn increase apoptotic load. Accumulation of lipids and cell debris in addition to proinflammatory cytokine production promotes lesion progression. In advanced, stiff lesions (**panel 3**), macrophage lipid uptake is also reduced, and increased lipid load in the environment creates cholesterol crystals which induce further inflammation and cytotoxicity. The increased apoptotic load is not efficiently cleared by macrophages (defective efferocytosis), contributing to secondary necrosis and the formation of a necrotic core. Increased matrix metalloprotease production leads to degradation and possible rupture of the fibrous cap (**panel 4**), releasing the toxic contents of the lesion into the lumen, where it induces platelet aggregation and thrombus formation.

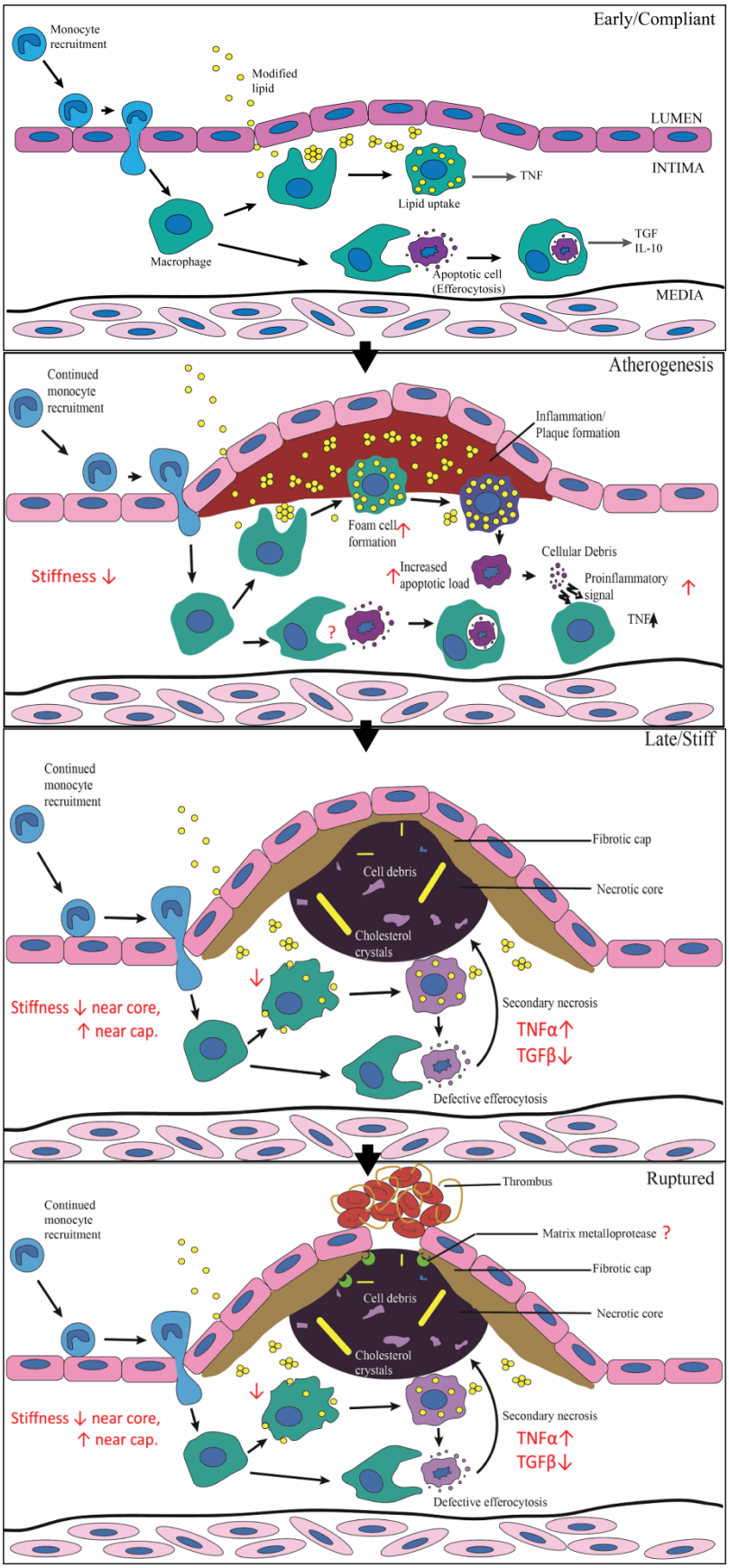
Early/Compliant
Monocyte recruitment
Modified lipid
LUMEN
INTIMA
TNF
Lipid uptake
Macrophage
TGF
IL-10
Apoptotic cell (Efferocytosis)
MEDIA
Atherogenesis
Continued monocyte recruitment
Inflammation/ Plaque formation
Foam cell formation
Stiffness ↓
Increased apoptotic load
Cellular Debris
Proinflammatory signal
TNF
?
Late/Stiff
Continued monocyte recruitment
Fibrotic cap
Cell debris
Necrotic core
Cholesterol crystals
Stiffness ↓ near core, ↑ near cap.
Secondary necrosis
TNFα↑
TGFβ↓
Defective efferocytosis
Ruptured
Thrombus
Continued monocyte recruitment
Matrix metalloprotease ?
Fibrotic cap
Cell debris
Necrotic core
Cholesterol crystals
Stiffness ↓ near core, ↑ near cap.
Secondary necrosis
TNFα↑
TGFβ↓
Defective efferocytosis

4.9 Model for Rho/ROCK/Integrin mechanism in macrophage mechanosensing

The mechanistic model of mechanosensing where integrin forms adhesions to ECM protein and signals actin cytoskeletal rearrangement is shown in **Figure 12.** Dynamic interactions of integrin heterodimers with ECM proteins exerts shear stress on the integrin molecule, activating the integrin dimer and initiating a signal cascade starting with the activation of focal adhesion kinase (FAK) and tyrosine protein kinase CSK (c-Src), phosphorylating signal adaptor proteins such as paxilin (PAX), cellular apoptosis susceptibility protein (CAS) and adapter molecule Crk (Shyy, 2002). Guanine exchange factors such as C3G convert the small GTPase RhoA to RhoA-GTP. This acts on ROCK, which inhibits myosin light chain (MLC) phosphatase and promotes MLC phosphorylation, increasing myosin II activity and causing shortening of actin fibers to form actin stress fibers (Maekawa, 1999). ROCK also activates LIM kinase (LIMK), which phosphorylates cofilin, inactivating its actin-depolymerization activity (Wang, 2009). Actin polymerizes to form filaments, which link to integrins via intermediaries such as paxilin, vinculin and talin, forming the focal adhesion complex.

ROCK1 is ubiquitously distributed in tissues and is the primary form of ROCK expressed in macrophages (Riento, 2003). It is therefore the primary form of ROCK that is responsible for mechanosensing in macrophages and thus would be important in modifying macrophage behavior.

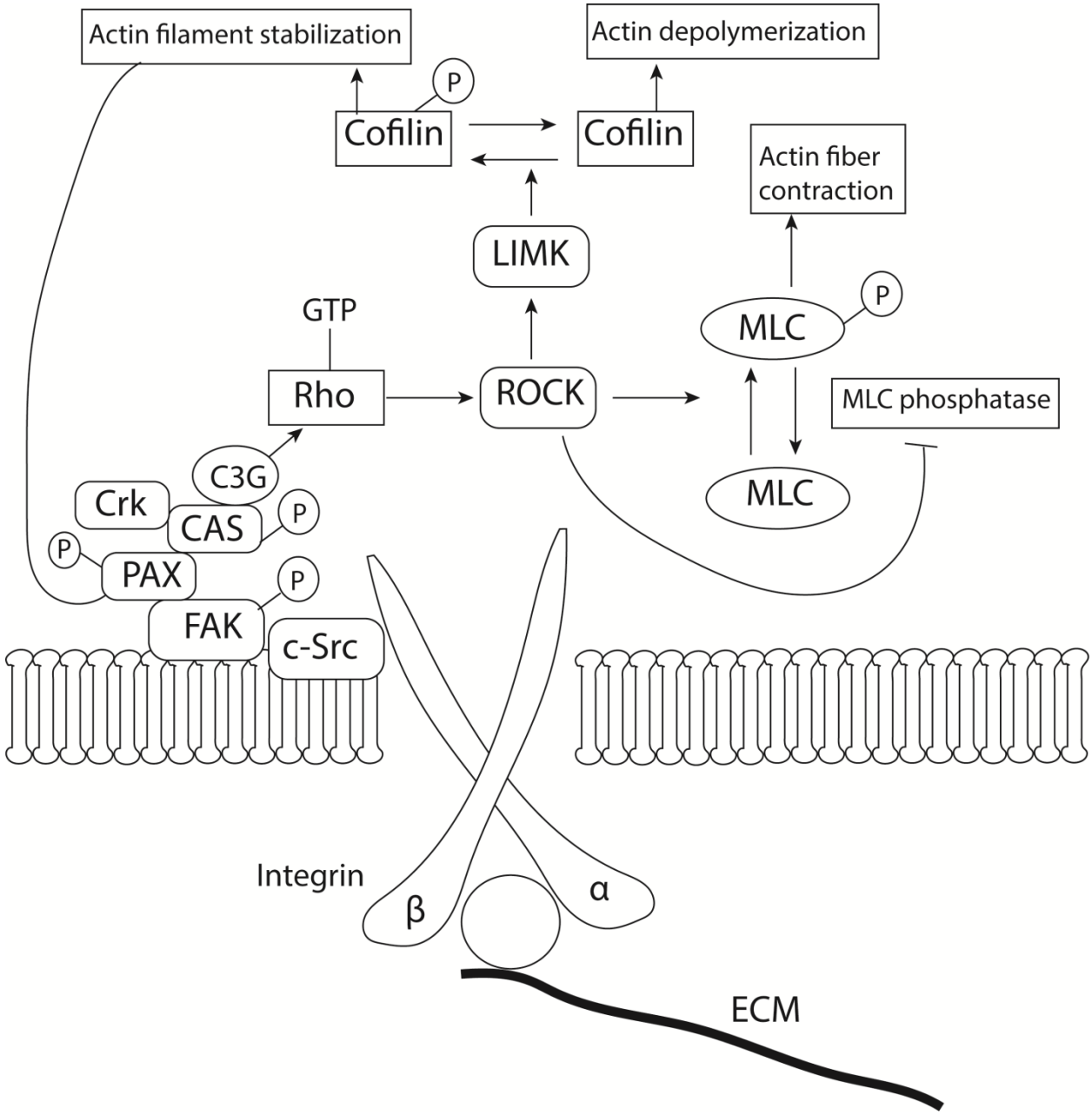

Figure 12: Mechanism of integrin stiffness signaling to ROCK via Rho. ECM proteins exert mechanical shear stress on inactive integrins, switching them to an active configuration. Specific interaction of the α-integrin with FAK and c-Src initiates the phosphorylation cascade of adaptor molecules (CAS, PAX, Crk) and guanine nucleotide exchange factors (C3G), phosphorylating Rho-GDP to Rho-GTP. Rho then acts on ROCK, which inhibits MLC phosphatase and promotes myosin light chain (MLC) phosphorylation, initiating actin fiber contraction. Additionally, ROCK activates LIM kinase, which phosphorylates cofilin, inactivating it and promoting actin filament stabilization. The actin filaments then attach to the integrin via paxilin to form the focal adhesion complex.

REFERENCES

1. Becker, L., Gharib, S.A., Irwin, A.D., Wijsman, E., Vaisar, T., Oram, J.F., and Heinecke, J.W. (2010). A macrophage sterol-responsive network linked to atherogenesis. Cell Metab.11, 125–135.

2. Blakney, A.K., Swartzlander, M.D., Bryant, S.J., (2012) The effects of substrate stiffness on the in vitro activation of macrophages and in vivo host response to poly (ethylene glycol) –based hydrogels. J Biomed. Mater. Res. A. 100(6), 1375-1386.

3. Brown, M.S., Ho, Y.K., and Goldstein, J.L. (1980). The cholesteryl ester cycle in macrophage foam cells. Continual hydrolysis and re-esterification of cytoplasmic cholesteryl esters. J. Biol. Chem.255, 9344–9352.

4. Brown, M.S., and Goldstein, J.L. (1997). The SREBP pathway: regulation of cholesterol metabolism by proteolysis of a membrane-bound transcription factor. Cell 89, 331–340.

5. Bubb, M.R., Senderowicz, A.M., Sausville, E.A., Duncan, K.L., Korn, E.D. (1994) Jasplakinolide, a cytotoxic natural product, induces actin polymerization and competitively inhibits the binding of phalloidin to F-actin. J. Biol. Chem. 269(21), 14869-14871.

6. Calkin, A.C., and Tontonoz, P. (2010). Liver x receptor signaling pathways and atherosclerosis. Arterioscler. Thromb. Vasc. Biol.30, 1513–1518.

7. Choudhary, S, Higgins, C.L., Chen, I.Y., Reardon, M., Lawrie, G., Vick, G.W., 3rd, Karmonik, C., Via, D.P., Morrisett, J.D. (2006) Quantitation and localization of matrix metalloproteinases and their inhibitors in human carotid endarterectomy tissues. Arterioscler Thromb Vasc Biol 26:2351-2358.

8. Chen LY, Zuraw BL, Liu FT, Huang S, Pan ZK. (2002) IL-1 receptor-associated kinase and low molecular weight GTPase RhoA signal molecules are required for bacterial lipopolysaccharide-induced cytokine gene transcription. J Immunol; 169: 3934–3939.

9. Chen LY, Doerner A, Lehmann PF, Huang S, Zhong G, Pan ZK. (2005) A novel protein kinase C (PKCepsilon) is required for fMet-Leu-Phe-induced activation of NFkappaB in human peripheral blood monocytes. J Biol Chem; 280: 22497–22501.

10. Curtiss, L.K., and Tobias, P.S. (2008). Emerging role of toll-like receptors in atherosclerosis. J. Lipid Res.50 Suppl., S340–S345.

11. deGoma, E.M., deGoma, R.L., and Rader, D.J. (2008). Beyond high-density lipoprotein cholesterol levels evaluating high-density lipoprotein function as influenced by novel therapeutic approaches. J. Am. Coll. Cardiol. 51, 2199–2211.

12. Duewell, P., Kono, H., Rayner, K.J., Sirois, C.M., Vladimer, G., Bauernfeind, F.G., Abela, G.S., Franchi, L., Nun˜ez, G., Schnurr, M., et al. (2010). NLRP3 inflammasomes are required for atherogenesis and activated by cholesterol crystals. Nature464, 1357–1361.

13. Engler, A.J., L Bacakova, C Newman, A Hategan, M Griffin, and D Discher (2004). Substrate compliance versus ligand density in cell on gel responses. Biophys J 86:617-628.

14. Engler, A.J., S Sen, HL Sweeney, and DE Discher. (2006) Matrix elasticity directs stem cell lineage specification. Cell 126:677-689.

15. Felton, CV, D Crook, MJ Davies, and MF Oliver (1997). Relation of plaque lipid composition and morphology to the stability of human aortic plaques. Arterioscler Thromb Vasc Biol 17:1337-1345.

16. Fereol S, Fodil R, Labat B, Galiacy S, Laurent VM, et al. (2006) Sensitivity of alveolar macrophages to substrate mechanical and adhesive properties. Cell Motil Cytoskeleton 63: 321–340.

17. Flannagan RS, Harrison RE, Yip CM, Jaqaman K, Grinstein S (2010) Dynamic macrophage "probing" is required for the efficient capture of phagocytic targets. J Cell Biol 191: 1205–1218.

18. Gareus, R., Kotsaki, E., Xanthoulea, S., van der Made, I., Gijbels, M.J., Kardakaris, R., Polykratis, A., Kollias, G., de Winther, M.P., and Pasparakis, M. (2008). Endothelial cell-specific NF-kappa inhibition protects mice from atherosclerosis. Cell Metab.8, 372–383.

19. Geissmann, F., Jung, S., Littman, D.R., (2003). Blood monocytes consist of two principal subsets with distinct migratory properties. Immunity 19(1), 71-82.

20. Glass, C.K., and Witztum, J.L. (2001). Atherosclerosis - the road ahead. Cell 104, 503–516.

21. Gillotte-Taylor, K., Nickel, M., Johnson, W.J., Francone, O.L., Holvoet, P., Lund-Katz, S., Rothblat, G.H., and Phillips, M.C. (2002). Effects of enrichment of fibroblasts with unesterified cholesterol on the efflux of cellular lipids to apolipoprotein A-I. J. Biol. Chem.277, 11811–11820.

22. Go AS, Mozaffarian D, Roger VL, Benjamin EJ, Berry JD, Blaha MJ, Dai S, Ford ES, Fox CS, Franco S, Fullerton HJ, Gillespie C, Hailpern SM, Heit JA, Howard VJ, Huffman MD, Judd SE, Kissela BM, Kittner SJ, Lackland DT, Lichtman JH, Lisabeth LD, Mackey R, Magid DJ, Marcus GM, Marelli A, Matchar DB, McGuire DK, Mohler ER 3rd, Moy CS, Mussolino ME, Neumar RW, Nichol G, Pandey DK, Paynter N, Reeves MJ, Sorlie PD, Stein J, Towfighi A, Turan TN, Virani SS, Wong ND, Woo D, Turner MB on behalf of the American Heart Association Statistics Committee and Stroke Statistics Subcommittee (2014). Heart disease and stroke statistics - 2014 update: a report from the American Heart Association. Circulation; 129:e28–e292.

23. Han, X., Kitamoto, S., Wang, H., and Boisvert, W.A. (2010). Interleukin-10 overexpression in macrophages suppresses atherosclerosis in hyperlipidemic mice. FASEB J.24, 2869–2880.

24. Henson, P.M., Bratton, D.L., and Fadok, V.A. (2001). Apoptotic cell removal. Curr. Biol.11, R795–R805.

25. Hughes, C.S.,Postovit, L.M., Lajoie, G.A. (2010). Matrigel: a complex protein mixture required for optimal growth of cell culture. Proteomics 10(9):1886-90

26. Huynh, J, N Nishimura, K Rana, JM Peloquin, JP Califano, CR Montague, MR King, CB Schaffer, and CA Reinhart-King (2011). Age-related intimal stiffening enhances endothelial permeability and leukocyte transmigration. Sci Transl Med 3:112ra122.

27. Huynh, ML, VA Fadok, and PM Henson. (2002) Phosphatidylserine-dependent ingestion of apoptotic cells promotes TGF-beta1 secretion and the resolution of inflammation. J Clin Invest 109:41-50.

28. Johnson, J.L., and Newby, A.C. (2009). Macrophage heterogeneity in atherosclerotic plaques. Curr. Opin. Lipidol.20, 370–378.

29. Kanters, E., Pasparakis, M., Gijbels, M.J., Vergouwe, M.N., Partouns-Hendriks, I., Fijneman, R.J., Clausen, B.E., Fo¨rster, I., Kockx, M.M., Rajewsky, K., et al. (2003). Inhibition of NF-kappa activation in macrophages increases atherosclerosis in LDL receptor-deficient mice. J. Clin. Invest.112, 1176–1185.

30. Kim, H.G., Kim, J.Y., Gim, M.G., Lee, J.M., Chung, D.K. (2008) Mechanical stress induces tumor necrosis factor (-alpha) production through Ca2+ release-dependent TLR2 signaling. Am J. Physiol. Cell Physiol. 295(2), C432-439.

31. Koenen, R.R., von Hundelshausen, P., Nesmelova, I.V., Zernecke, A., Liehn, E.A., Sarabi, A., Kramp, B.K., Piccinini, A.M., Paludan, S.R., Kowalska, M.A., et al. (2009). Disrupting functional interactions between platelet chemokines inhibits atherosclerosis in hyperlipidemic mice. Nat. Med. 15, 97–103.

32. Leung T, et al. (1996) The p160 RhoA-binding kinase ROK alpha is a member of a kinase family and is involved in the reorganization of the cytoskeleton. Mol Cell Biol. 16:5313–5327.

33. Li, S., Sun, Y., Liang, C.P., Thorp, E.B., Han, S., Jehle, A.W., Saraswathi, V., Pridgen, B., Kanter, J.E., Li, R., et al. (2009). Defective phagocytosis of apoptotic cells by macrophages in atherosclerotic lesions of ob/ob mice and reversal by a fish oil diet. Circ. Res.105, 1072–1082.

34. Li, Y, MC Gerbod-Giannone, H Seitz, D Cui, E Thorp, AR Tall, GK Matsushima, and I Tabas. (2006) Cholesterol-induced apoptotic macrophages elicit an inflammatory response in phagocytes, which is partially attenuated by the Mer receptor. J Biol Chem 281:6707-6717.

35. Loirand, G., Guilluy, C., Pacaud, P., (2006). Regulation of Rho proteins by phosphorylation in the cardiovascular system. Trends Cardiovasc. Med. 16(6), 199-204.

36. Lundberg, A.M., Ketelhuth, D.F.J., Johansson, M.E., Gerdes, N., Liu, S., Yamamoto, M., Akira, S., Hansson, G.K. (2013). Toll-like receptor 3 and 4 signaling through the TRIF and TRAM adaptors in haematopoietic cells promotes atherosclerosis. Cardiovasc. Res., 99:364-373

37. Lutgens, E., Lievens, D., Beckers, L., Wijnands, E., Soehnlein, O., Zernecke, A., Seijkens, T., Engel, D., Cleutjens, J., Keller, A.M., et al. (2010). Deficient CD40-TRAF6 signaling in leukocytes prevents atherosclerosis by skewing the immune response toward an anti-inflammatory profile. J. Exp. Med. 207, 391–404.

38. Maekawa M, Ishizaki T, Boku S, *et al.*(1999). Signaling from Rho to the actin cytoskeleton through protein kinases ROCK and LIM-kinase. Science 285 (5429): 895–8.

39. Mantovani, A., Sica, A., Sozzani, S., Allavena, P., Vecchi, A., Locati, M. (2004) The chemokine system in diverse forms of macrophage activation and polarization. Trends Immun. 25(12), 677-686.

40. Mantovani, A, C Garlanda, and M Locati (2009). Macrophage diversity and polarization in atherosclerosis: a question of balance. Arterioscler Thromb Vasc Biol 29:1419-1423.

41. Maxfield, F.R., and Tabas, I. (2005). Role of cholesterol and lipid organization in disease. Nature438, 612–621.

42. Mestas, J., and Ley, K. (2008). Monocyte-endothelial cell interactions in the development of atherosclerosis. Trends Cardiovasc. Med.18, 228–232.

43. Michelsen, K.S., Wong, M.H., Shah, P.K., Zhang, W., Yano, J., Doherty, T.M., Akira, S., Rajavashisth, T.B., Arditi, M. (2004). Lack of toll-like receptor 4 or myeloid differentiation factor 88 reduces atherosclerosis and alters plaque phenotype in mice deficient in apolipoprotein E.Proc. Natl. Acad. Sci. U.S.A., 101: 10679–10684.

44. Moore, K.J. & Tabas, I. (2011) Macrophages in the pathogenesis of atherosclerosis.Cell145, 341–355.

45. Mullick, A.E., Tobias, P.S., and Curtiss, L.K. (2005). Modulation of atherosclerosis in mice by Toll-like receptor 2. J. Clin. Invest.115, 3149–3156.

46. Nagase, H, Visse, R., Murphy, G. (2006) Structure and function of matrix metalloproteinases and TIMPs. Cardiovasc Res 69:562-573.

47. Newby, A.C. (2007) Metalloproteinases and vulnerable atherosclerotic plaques. Trends Cardiovasc Med 17:253-258.

48. Oka, T., Hikoso, S., Yamaguchi, O., Taneike, M., Takeda, T., Tamai, T., Oyabu, J., Murakawa, T., Nakayama, H., Nishida, K., Akira, S., Yamamoto, A., Komuro, I., Otsu, K. (2012). Mitochondrial DNA that escapes from autophagy causes inflammation and heart failure. Nature, 485: 251–255

49. Patel, NR, M Bole, C Chen, CC Hardin, AT Kho, J Mih, L Deng, J Butler, D Tschumperlin, JJ Friedberg, R Krishnan, and H Kossel. (2012) Cell elasticity determines macrophage function. Plops One 7:e41024.

50. Paulson, K.E., Zhu, S.N., Chen, M., Nurmohamed, S., Jongstra-Bilen, J., and Cybulsky, M.I. (2010). Resident intimal dendritic cells accumulate lipid and contribute to the initiation of atherosclerosis. Circ. Res.106, 383–390.

51. Pelham, RJ, Jr., and Y Wang. (1997) Cell locomotion and focal adhesions are regulated by substrate flexibility. Proc Natl Acad Sci. USA 94:13661-13665.

52. Rajamäki, K., Lappalainen, J., Oo¨rni, K., Va ¨lima ¨ki, E., Matikainen, S., Kovanen, P.T., and Eklund, K.K.; Ref Type. (2010). Cholesterol crystals activate the NLRP3 inflammasome in human macrophages: a novel link between cholesterol metabolism and inflammation. PLoS ONE5, e11765.

53. Rajavashisth, T, JH Qiao, S Tripathi, J Tripathi, N Mishra, M Hua, XP Wang, A Loussararian, S Clinton, P Libby, and A Lusis. (1998) Heterozygous osteopetrotic (op) mutation reduces atherosclerosis in LDL receptor- deficient mice. J Clin Invest 101:2702-2710.

54. Ramirez-Ortiz, Z.G., Specht, C.A., Wang, J.P., Lee, C.K., Bartholomeu, D.C., Gazzinelli, R.T., Levitz, S.M. (2008). Toll-Like Receptor 9-Dependent Immune Activation by Unmethylated CpG Motifs in *Aspergillus fumigates* DNA. Infect. Immun. 76(5):2123-2129/

55. Riento K, Ridley AJ (2003). Rocks: multifunctional kinases in cell behaviour. Nat. Rev. Mol. Cell Biol. 4 (6): 446–56.

56. Rothblat, G.H., and Phillips, M.C. (2010). High-density lipoprotein heterogeneity and function in reverse cholesterol transport. Curr. Opin. Lipidol.21, 229–238.

57. Salagianni, M., Galani, I.E., Lundberg, A.M., Davos, C.H., Varela, A., Gavriil, A., Lyytikäinen, L.P., Lehtimäki, T., Sigala, F., Folkersen, L., Gorgoulis, V., Lenglet, S., Montecucco, F., MacH, F., Hedin, U., Hansson, G.K., Monaco, C., Andreakos, E. (2012). Toll-like receptor 7 protects from atherosclerosis by constraining inflammatory macrophage activation. Circulation, 126:952–962.

58. Sather, S., Kenyon, K.D., Lefkowitz, J.B., Liang, X., Varnum, B.C., Henson, P.M., and Graham, D.K. (2007). A soluble form of the Mer receptor tyrosine kinase inhibits macrophage clearance of apoptotic cells and platelet aggregation. Blood109, 1026–1033.

59. Scott, V.R., Boehme, R., Matthews, T.R. (1988). New class of antifungal agents: Jasplakinolide, a cyclodepsipeptide from the marine sponge, Jaspis species. Antimicrob. Agents Chemother. 32(8), 1154-1157.

60. Shibata, N., and Glass, C.K. (2009). Regulation of macrophage functions in inflammation and atherosclerosis. J. Lipid Res. Suppl. 50, S277–S281.

61. Shih, YR, KF Tseng, HY Lai, CH Lin, and OK Lee. (2011) Matrix stiffness regulation of integrinmediated mechanotransduction during osteogenic differentiation of human mesenchymal stem cells. J Bone Miner Res 26:730-738.

62. Shimokawa, H., Rashid, M., (2007). Development of Rho-kinase inhibitors for cardiovascular medicine. Trends Pharmacol. Sci. 2007 28(6), 296-302.

63. Shyy, J.Y.J., Chien, S. (2002). Role of Integrins in Endothelial Mechanosensing of Shear Stress. Circ. Res, 91:769-775

64. Smith, JD, E Trogan, M Ginsberg, C Grigaux, J Tian, and M Miyata. (1995) Decreased atherosclerosis in mice deficient in both macrophage colony-stimulating factor (op) and apolipoprotein E. Proc Natl Acad Sci USA 92:8264-8268.

65. Somlyo AP, Somlyo AV. (2000) Signal transduction by G-proteins, rho-kinase and protein phosphatase to smooth muscle and non-muscle myosin II. J Physiol.;522(2):177–185.

66. Stewart, C.R., Stuart, L.M., Wilkinson, K., van Gils, J.M., Deng, J., Halle, A., Rayner, K.J., Boyer, L., Zhong, R., Frazier, W.A., et al. (2010). CD36 ligands promote sterile inflammation through assembly of a Toll-like receptor 4 and 6 heterodimer. Nat. Immunol.11, 155–161.

67. Stoger, JL, P Goossens, and MP de Winther. (2010) Macrophage heterogeneity: relevance and functional implications in atherosclerosis. Curr Vasc Pharmacol 8:233-248.

68. Stout, R.D., Suttles, J. (2004) Functional plasticity of macrophages: reversible adaptation to changing microenvironments. J. Leukoc. Biol. 76(3), 509-513.

69. Tabas, I. (2010). Macrophage death and defective inflammation resolution in atherosclerosis. Nat. Rev. Immunol.10, 36–46.

70. Tall, A.R., Yvan-Charvet, L., Terasaka, N., Pagler, T., and Wang, N. (2008). HDL, ABC transporters, and cholesterol efflux: implications for the treatment of atherosclerosis. Cell Metab.7, 365–375.

71. Tang, C., Liu, Y., Kessler, P.S., Vaughan, A.M., and Oram, J.F. (2009). The macrophage cholesterol exporter ABCA1 functions as an anti-inflammatory receptor. J. Biol. Chem.284, 32336–32343.

72. Tracqui, P., Broisat, A., Toczek, J., Mesnier, N., Ohayon, J., Riou, L.(2011) Mapping elasticity moduli of atherosclerotic plaque in situ via atomic force microscopy. J Struct Biol 174:115-123.

73. Tosello-Trampont, AC, K Nakada-Tsukui, and KS Ravichandran (2003). Engulfment of apoptotic cells is negatively regulated by Rho-mediated signaling. J Biol Chem 278:49911-49919.

74. Uehata, M; Ishizaki, T; Satoh, H; Ono, T; Kawahara, T; Morishita, T; Tamakawa, H; Yamagami, K et al. (1997). Calcium sensitization of smooth muscle mediated by a Rho-associated protein kinase in hypertension. *Nature* **389** (6654): 990–994.

75. Van Goethem, E, R Poincloux, F Gauffre, I Maridonneau-Parini, and V Le Cabec. (2010) Matrix architecture dictates three-dimensional migration modes of human macrophages: differential involvement of proteases and podosome-like structures. J Immunol 184:1049-1061.

76. Vedhachalam, C., Duong, P.T., Nickel, M., Nguyen, D., Dhanasekaran, P., Saito, H., Rothblat, G.H., Lund-Katz, S., and Phillips, M.C. (2007). Mechanism of ATP-binding cassette transporter A1-mediated cellular lipid efflux to apolipoprotein A-I and formation of high density lipoprotein particles. J. Biol. Chem. 282, 25123–25130.

77. Visegrady, B., Lorinczy, D., Hild, G., Somogyi, B., Nyitrai, M. (2005) A simple model for the cooperative stabilization of actin filaments by phalloidin and Jasplakinolide. FEBS Lett. 579(1), 6-10.

78. Virmani, R., Burke, A.P., Kolodgie, F.D., and Farb, A. (2002). Vulnerable plaque: the pathology of unstable coronary lesions. J. Interv. Cardiol. 15,439–446.

79. Vonna L, Wiedemann A, Aepfelbacher M, Sackmann E (2007) Micromechanics of filopodia mediated capture of pathogens by macrophages. Eur Biophys J 36: 145–151.

80. Wang, HW, PY Liu, N Oyama, Y Rikitake, S Kitamoto, J Gitlin, JK Liao, and WA Boisvert. (2008) Deficiency of ROCK1 in bone marrow-derived cells protects against atherosclerosis in LDLR-/- mice. FASEB J 22:3561-3570.

81. Wang, N., Lan, D., Chen, W., Matsuura, F., and Tall, A.R. (2004). ATP-binding cassette transporters G1 and G4 mediate cellular cholesterol efflux to high density lipoproteins. Proc. Natl. Acad. Sci. USA101, 9774–9779.

82. Wang, N., Ranalletta, M., Matsuura, F., Peng, F., and Tall, A.R. (2006). LXR-induced redistribution of ABCG1 to plasma membrane in macrophages enhances cholesterol mass efflux to HDL. Arterioscler. Thromb. Vasc. Biol. 26, 1310–1316.

83. Wang Y, Zheng XR, Riddick N, *et al* .(2009). ROCK Isoform Regulation of Myosin Phosphatase and Contractility in Vascular Smooth Muscle Cells. *Circ. Res.* 104 (4): 531–40.

84. Wilensky, R.L., and Macphee, C.H. (2009). Lipoprotein-associated phospholipase A(2) and atherosclerosis. Curr. Opin. Lipidol.20, 415–420.

85. Williams, K.J., and Tabas, I. (1995). The response-to-retention hypothesis of early atherogenesis. Arterioscler. Thromb. Vasc. Biol.15, 551–561.

86. Wong, J., Quinn, C.M., Gelissen, I.C., Jessup W., Brown, A.J. (2008). The effect of statins on ABCA1 and ABCG1 expression in human macrophages is influenced by cellular cholesterol levels and extent of differentiation. Atheroscl.196. 180-189.

87. Yvan-Charvet, L., Ranalletta, M., Wang, N., Han, S., Terasaka, N., Li, R.,Welch, C., and Tall, A.R. (2007). Combined deficiency of ABCA1 and ABCG1 promotes foam cell accumulation and accelerates atherosclerosis in mice. J. Clin. Invest.117, 3900–3908.

88. Yvan-Charvet, L., Pagler, T.A., Seimon, T.A., Thorp, E., Welch, C.L., Witztum, J.L., Tabas, I., and Tall, A.R. (2010). ABCA1 and ABCG1 protect against oxidative stress-induced macrophage apoptosis during efferocytosis. Circ. Res.106, 1861–1869.

89. Zhou, Q., Gensch, C., Liao, G.K. (2011). Rho-associated coiled-coil-forming kinases (ROCKs): potential targets for the treatment of atherosclerosis and vascular disease. Trends Pharmacol. Sci. 32(3), 167-173.

90. Zhu, X., Lee, J.Y., Timmins, J.M., Brown, J.M., Boudyguina, E., Mulya, A., Gebre, A.K., Willingham, M.C., Hiltbold, E.M., Mishra, N., et al. (2008). Increased cellular free cholesterol in macrophage-specific Abca1 knock-out mice enhances pro-inflammatory response of macrophages. J. Biol. Chem.283, 22930–22941.